表 4. 免疫学的評価と臨床効果

症例	CpG Dose (mg/kg)	PS	CTL response (ELISPOT) URLC10	CTL response (ELISPOT) TTK	CTL frequency (Pentamer) URLC10	CTL frequency (Pentamer) TTK	臨床効果
1	—	1	−	−	NT	NT	PD
2	—	0	+	−	+	−	SD
3	—	1	+	−	−	−	PD
4	0.02	1	+	++	+	−	PD
5	0.02	0	−	−	+	−	SD
6	0.02	1	+++	−	+++	−	SD
7	0.1	1	−	−	−	−	SD
8	0.1	0	+++	−	+++	−	SD
9	0.1	1	+	+	NT	NT	PD

NT：not tested

（岩橋誠ほか，2010[17]より引用）

にCpG[15]を併用する，ペプチドワクチン療法の第Ⅰ相試験である[16][17]．免疫学的評価では，9例中6例でURLC10に対する，9例中2例でTTKに対する抗原特異的反応を認め，とくにCpG-B併用例においてより強力な免疫反応が誘導されていた[18]．臨床効果ではとくにCpG-B併用6例中4例がstable disease（SD）であり，うち1例は12ヵ月以上の長期間SDを持続した（表4）．現在，臨床的有効性を評価する第Ⅱ相試験が進行中である．

もう1つは，切除不能進行再発膵がんに対する腫瘍新生血管を標的としたVEGR2由来のエピトープペプチド[19]とGEM併用による第Ⅰ相試験である[3]．有害事象はGEM単独投与例と差は認めなかった．免疫学的評価ではGEM併用にもかかわらず，18例中11例（61%）にCTLが誘導されていた．またCTL反応を認めた11例において，ワクチン投与前後で末梢血単核球（peripheral blood mononuclear cell：PBMC）中の制御性T細胞（regulatory T cell：Treg）分画比率の減少を認めた．注射部位反応は15例（83%）に認めたが，このうちpartial response（PR）またはSDを認めた症例は12例であり，progressive disease（PD）は3例のみであった．一方，注射部位反応を認めなかった3例はすべてPDであり，注射部位反応と臨床効果が相関することが示唆された（表5）．臨床効果はResponse Evaluation Criteria in Solid Tumors（RECIST）評価ではPR 1例，SD 11例でdisease control rateは67%であった．生存期間中央値（median survival time：MST）は7.7ヵ月であり，前治療のない15例のMSTは8.7ヵ月と良好であった（図1）．推奨投与量の決定に関しては，毒性の観点からは決定に至らなかった．免疫学的観点からは，CTL反応と臨床効果に相関する注射部位反応が高率に認められた2.0 mg/bodyを推奨投与量とした．

このGEM＋VEGFR2エピトープペプチドの医師主導型臨床試験結果を受け，2009年1月から全国27施設の参加を得て企業主導の臨床治験（OTS102）として第Ⅱ/Ⅲ相試験（PEGASUS-PC試験）が開始された．2010年1月で153例の症例登録が終了し，2010年11月の効果安全性評価委員会での中間解析の結果，試験継続の勧告を受け，

表 5. 免疫学的評価と臨床効果

	gender	age	reaction at the injection site	CTL respose	Best overall response	Dead/alive	Survival (day)
0.5 mg/body							
Cohort Ⅰ	F	68	(−)	(−)	PD	Dead	102
	M	64	(+)	(+)	SD	Dead	222
	M	61	(+)	(+)	SD	Dead	232
	F	38	(+)	(−)	SD	Dead	304
	M	75	(+)	(+)	PD	Dead	233
	M	72	(+)	(−)	SD	Dead	334
1.0 mg/body							
Cohort Ⅱ	M	65	(−)	(+)	PD	Dead	135
	F	57	(+)	(+)	SD	Dead	548
	M	69	(+)	(−)	SD	Dead	880
	M	79	(+)	(−)	SD	Dead	185
	M	56	(+)	(+)	SD	Dead	229
	M	67	(−)	(+)	PD	Dead	143
2.0 mg/body							
Cohort Ⅲ	M	58	(+)	(+)	PD	Dead	109
	M	62	(+)	(+)	PR	Dead	835
	M	78	(+)	(+)	SD	Dead	1088
	F	64	(+)	(−)	SD	Dead	265
	M	64	(+)	(−)	SD	Dead	605
	M	65	(+)	(+)	PD	Dead	536

＊ Clinical improvement

(Miyazawa M *et al*, 2010[9]より改変引用)

現在，追跡調査中である．2012年2月には最終結果が報告される予定であるが（執筆時），本治験はわが国初のがんワクチン療法の pivotal study であり，その結果により承認に至れば世界初のペプチドワクチン薬となる．

6 わが国におけるがんワクチン療法開発の問題点

本稿で示したように，現在，わが国では医師主導臨床試験，さらに企業治験をとおしてがんワクチン療法の承認をめざした開発が進行中であるが，現在まで医薬品として厚生労働省の承認を受

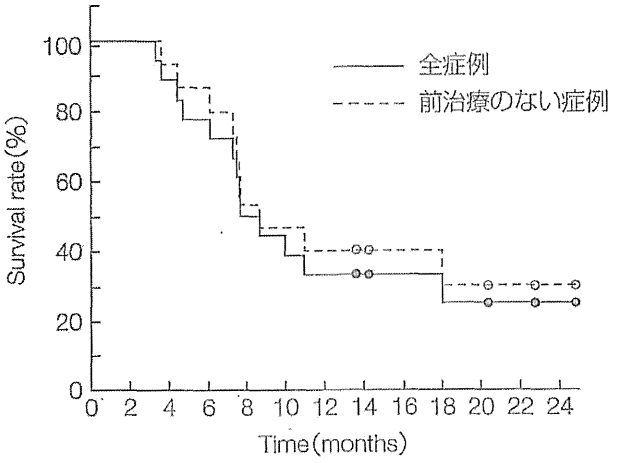

図 1. VEGFR2 由来エピトープペプチドワクチン療法＋GEM の生存期間
18 例全例の MST は 7.7ヵ月であり，前治療のない 15 例の MST は 8.7ヵ月であった．
（Miyazawa M *et al*, 2010[3] より改変引用）

けた治療はまだない．今後，現在開発中のいくつかの薬剤（ペプチドなど）が承認されていくことを期待するが，国の開発・承認にあたっての考え方が明確にされていないのが現状である．一方，米国では前述したように FDA ががんワクチンの開発を進める企業に対しガイダンスを出して，考え方を明確に示している[6]．現在まで，わが国においては厚生労働省や医薬品医療機器総合機構（Pharmaceuticals and Medical Devices Agency：PMDA）からそのような動きはみられていない．しかしながら，がんワクチン開発の世界的な動向からみてもこの点は非常に重要と考えられる．そのような状況のなか，日本バイオセラピィ学会は 2011 年 11 月に「がん治療用ペプチドワクチンガイダンス（案）」[8]を作成し，第 24 回日本バイオセラピィ学会学術集会総会（2011 年 12 月，和歌山市）で特別企画としてがん治療用ペプチドワクチンガイダンス公聴会を開催した．今後，本会を通じ広くパブリックコメントを募集し，本格的なガイダンス作成に取り組んでいくことになっている．

おわりに

国際的にはがんワクチン療法は外科手術，化学療法，放射線治療につぐ新たな治療として注目され，すでに承認に至っている．この分野での治療開発が加速しており，近い将来更なる治療薬が生まれる状況にある．一方，わが国においてもがんワクチン療法，とくにペプチドワクチン療法が創薬に向かって企業治験が開始された．近日中にその一部の結果が報告される予定であり，わが国初のがんワクチン療法の承認に向け，将来の発展が期待される．そのなかで多くの研究者は，ワクチンの効果が最も期待できるであろう術後アジュバントを対象にした臨床試験が計画されることを望んでいる．しかし，この領域では結果を得るのに大変な時間と費用を要するため，開発を進める企業として多大なリスクを強いられる．しかし，ワクチンの本来の予防という観点から，がんワクチンは再発予防にこそその効力が発揮されると考えられる．したがって，このような領域にこそ国の支援が得られることを大いに期待したい．

文　献

1) Rosenberg SA, Yang JC, Restifo NP：Cancer immunotherapy：moving beyond current vaccines. *Nat Med* **10**：909-915, 2004
2) Cheever MA, Higano CS：PROVENGE (Sipuleucel-T) in prostate cancer：the first FDA-approved therapeutic cancer vaccine. *Clin Cancer Res* **17**：3520-3526, 2011
3) Miyazawa M, Ohsawa R, Tsunoda T *et al*：Phase I clinical trial using peptide vaccine for human vascular endothelial growth factor receptor 2 in combination with gemcitabine for patients with advanced pancreatic cancer. *Cancer Sci* **101**：433-439, 2010
4) van der Bruggen P, Traversari C, Chomez P *et al*：A gene encoding an antigen recognized by cytolytic T lymphocytes on a human melanoma. *Science* **254**：1643-1647, 1991
5) 池田裕明，珠玖洋：CD8＋細胞傷害性 T 細胞の制

御による抗腫瘍免疫増強—養子免疫療法・タンパク質ワクチン—. 実験医 **27**：2176-2184, 2009
6) Draft Guidance for industry：Clinical considerations for therapeutic cancer vaccines. U.S. Department of Health and Human Services Food and Drug Administration Center for Biologics Evaluation and Research, 2009
7) Zucker DM, Yang S：Inference for a family of survival models encompassing the proportional hazards and proportional odds models. *Stat Med* **25**：995-1014, 2006
8) 日本バイオセラピィ学会 がん治療用ペプチドワクチンガイダンス（案），日本バイオセラピィ学会 がん治療用ペプチドワクチンガイダンス委員会編，http://www5.ocn.ne.jp/~jbt/guideline.html
9) Oka Y, Tsuboi A, Murakami M *et al*：Wilms tumor gene peptide-based immunotherapy for patients with overt leukemia from myelodysplastic syndrome (MDS) or MDS with myelofibrosis. *Int J Hematol* **78**：56-61, 2003
10) Kawada J, Wada H, Isobe M *et al*：Heteroclitic serological response in esophageal and prostate cancer patients after NY-ESO-1 protein vaccination. *Int J Cancer* **130**：584-592, 2012
11) 吉田浩二，中村祐輔：消化器癌に対するがんペプチドワクチン療法. 日消誌 **107**：1255-1261, 2010
12) Noguchi M, Mine T, Komatsu N *et al*：Assessment of immunological biomarkers in patients with advanced cancer treated by personalized peptide vaccination. *Cancer Biol Ther* **10**：1266-1279, 2011
13) Kono K, Mizukami Y, Daigo Y *et al*：Vaccination with multiple peptides derived from novel cancer-testis antigens can induce specific T-cell responses and clinical responses in advanced esophageal cancer. *Cancer Sci* **100**：1502-1509, 2009
14) Suda T, Tsunoda T, Uchida N *et al*：Identification of secernin 1 as a novel immunotherapy target for gastric cancer using the expression profiles of cDNA microarray. *Cancer Sci* **97**：411-419, 2006
15) Speiser DE, Liénard D, Rufer N *et al*：Rapid and strong human $CD8^+$ T cell responses to vaccination with peptide, IFA, and CpG oligodeoxynucleotide 7909. *J Clin Invest* **115**：739-746, 2005
16) Iwahashi M, Katsuda M, Nakamori M *et al*：Vaccination with peptides derived from cancer-testis antigens in combination with CpG-7909 elicits strong specific CD8+ T cell response in patients with metastatic esophageal squamous cell carcinoma. *Cancer Sci* **101**：2510-2517, 2010
17) 岩橋誠，勝田将裕，中森幹人ほか：進行食道癌に対するCpG-B併用新規腫瘍抗原ペプチドワクチン療法. *Biotherapy* **24**：375-380, 2010
18) Katsuda M, Iwahashi M, Matsuda K *et al*：Comparison of different classes of CpG-ODN in augmenting the generation of human epitope peptide-specific CTLs. *Int J Oncol* **39**：1295-1302, 2011
19) Wada S, Tsunoda T, Baba T *et al*：Rationale for antiangiogenic cancer therapy with vaccination using epitope peptides derived from human vascular endothelial growth factor receptor 2. *Cancer Res* **65**：4939-4946, 2005

Pylorus Ring Resection Reduces Delayed Gastric Emptying in Patients Undergoing Pancreatoduodenectomy

A Prospective, Randomized, Controlled Trial of Pylorus-Resecting Versus Pylorus-Preserving Pancreatoduodenectomy

Manabu Kawai, MD, Masaji Tani, MD, Seiko Hirono, MD, Motoki Miyazawa, MD, Atsushi Shimizu, MD, Kazuhisa Uchiyama, MD, and Hiroki Yamaue, MD

Objective: To determine in a prospective randomized controlled trial (RCT) whether pylorus-resecting pancreatoduodenectomy (PrPD) with preservation of nearly the entire stomach reduces the incidence of delayed gastric emptying (DGE) compared with pylorus-preserving pancreatoduodenectomy (PpPD).

Background: Several RCTs have compared PpPD and conventional pancreatoduodenectomy with antrectomy. However, no study has reported the difference between PrPD with preservation of nearly the entire stomach and PpPD.

Methods: One hundred thirty patients were randomized to preservation of the pylorus ring (PpPD) or to resection of the pylorus ring with preservation of nearly the entire stomach (PrPD). This RCT was registered at clinicaltrials.gov NCT00639314.

Results: The incidence of DGE was 4.5% in PrPD and 17.2% in PpPD, a significant difference. Delayed gastric emptying was classified into 3 categories proposed by the International Study Group of Pancreatic Surgery. The proposed clinical grading classified 11 cases of DGE in PpPD into grades A (n = 6), B (n = 5), and C (n = 0) and one case in PrPD into each of the 3 grades. The time to peak $^{13}CO_2$ content in the ^{13}C-acetate breath test at 1, 3, and 6 months postoperatively was significantly delayed in PpPD compared with PrPD (34.3 ± 24.6 minutes versus 18.7 ± 11.8 minutes, 26.5 ± 21.1 minutes versus 17.3 ± 11.7 minutes, 26.7 ± 18.8 minutes versus 17.4 ± 13.2 minutes, respectively). Pylorus-resecting pancreatoduodenectomy and PpPD had comparable outcomes for quality of life, weight loss, and nutritional status during a 6-month follow-up period.

Conclusion: Pylorus-resecting pancreatoduodenectomy significantly reduces of the incidence of DGE compared with PpPD.

(*Ann Surg* 2011;253:495–501)

Pylorus-preserving pancreatoduodenectomy (PpPD) with preservation of the entire stomach was popularized for the treatment of chronic pancreatitis as a modification of conventional pancreatoduodenectomy (PD) with antrectomy reported by Traverso and Longmire[1] in the late 1970s. Results of several randomized controlled trials (RCTs) or meta-analyses comparing PpPD and PD have been reported, and the 2 procedures are equivalent in regard to morbidity, mortality, and survival for the treatment of periampullary tumors.[2–7] Moreover, PpPD has been reported to reduce dumping, diarrhea, and bile reflux gastritis after gastrectomy and to afford patients an improved nutritional status compared with PD with antrectomy.[8–12] Therefore, PpPD has been generally accepted as the surgical procedure for periampullary neoplasms such as cancer of the pancreatic head or bile duct.

However, delayed gastric emptying (DGE) after PpPD is a persistent and frustrating complication. Delayed gastric emptying, with an incidence varying from 12% to 42% in previous series, is not a life-threatening complication, but it results in a prolonged length of stay that contributes to increased hospital costs and decreased quality of life (QOL).[12–16]

The pathogenesis of DGE after PpPD remains controversial. Delayed gastric emptying after PpPD has been attributed to denervation and devascularization of the pylorus ring due to pylorospasm caused by operative injuries of the vagus nerves innervating the pyloric ring,[17–19] ischemia of the pylorus ring due to division of the right gastric artery,[20] or congestion around the pylorus ring due to division of the left gastric vein.[21] Therefore, one should consider developing a new PD surgical procedure with resection of only the pylorus ring with preservation of nearly all the stomach. To our knowledge, no report has evaluated whether resection of the pylorus ring in PD lowers the incidence of DGE compared with that in PpPD. We designed this technique to preserve more than 95% of the stomach, calling the procedure pylorus-resecting pancreatoduodenectomy (PrPD). We conducted this RCT to confirm the hypothesis that PrPD reduces the incidence of DGE compared with conventional PpPD.

PATIENTS AND METHODS

Between October 2005 and March 2009, this RCT was performed at Wakayama Medical University Hospital (WMUH) to compare PrPD and PpPD in patients with pancreatic or periampullary lesions. A total of 139 eligible patients were recruited into the study before surgery on the basis of whether preserving the pylorus ring was anticipated. This trial was approved by the Ethical Committee on Clinical Investigation of WMUH and prepared in accordance with clinicaltrials.gov (ID# NCT00639314). Informed consent was obtained from all participating patients preoperatively; they also agreed to a follow-up of at least 6 months postoperatively. Exclusion criteria were (1) tumor infiltration into the stomach and metastasis into lymph nodes of the peripylorus; (2) patients with severe comorbidity such as myocardial infarction, respiratory disorder that required oxygen inhalation, liver cirrhosis, hemodialysis, or cancer of the other organ, which were possible to prolong hospital stay; (3) patients with combined resection of the liver; (4) patients with proven mental illness; and (5) patients without an informed consent.

Assignment

During PD, patients were randomized to the group with preservation of the pylorus ring (PpPD) or resection of the pylorus ring with preservation of more than 95% of the stomach (PrPD). A research physician conducted the randomization using a computer-generated random number pattern in a central registry for the study at WMUH.

From the Second Department of Surgery, Wakayama Medical University School of Medicine, Wakayama, Japan.

This study was registered at clinicaltrials.gov; ID# NCT00639314.

Reprints: Hiroki Yamaue, MD, Second Department of Surgery, Wakayama Medical University, School of Medicine, 811-1 Kimiidera, Wakayama 641, Japan. E-mail: yamaue-h@wakayama-med.ac.jp.

ISSN: 0003-4932/11/25303-0495
DOI: 10.1097/SLA.0b013e31820d98f1

Description of the Operations

Figure 1 presents a schematic drawing of the 2 procedures. The root of the right gastric artery and the pyloric branch of the vagal nerve were dissected at the same levels along with lymph nodes around the pylorus ring in both PpPD and PrPD. In PpPD, the proximal duodenum was divided 3 to 4 cm distal to the pylorus ring. In PrPD, the stomach was divided just adjacent to the pylorus ring and more than 95% of the stomach was preserved. In patients with malignant disease, for either procedure, lymph nodes from the following areas were removed: hepatoduodenal ligament, circumferentially around the common hepatic artery, and the right-half circumference of the superior mesenteric artery.

All patients underwent PD with the following reconstruction.[22] Pancreatojejunostomy after PpPD and PrPD was performed by duct-to-mucosa, end-to-side pancreatojejunostomy in all patients.[23] External suture rows were created as a single suture between the remnant pancreatic capsule, parenchyma, and jejunal seromuscular tissue by using interrupted sutures of 4-0 Novafil (polybutester, Tyco Healthcare Japan Co, Tokyo, Japan). Internal suture rows, duct to mucosa, were performed between the pancreatic duct and jejunal mucosa by using 8 interrupted 5-0 PDS-II (polydioxanone, Johnson and Johnson Co, Tokyo, Japan). The internal drainage catheter, cut to a length of 5 cm of a 5-F polyethylene pancreatic duct drainage catheter (Sumitomo Bakelite Co, Tokyo, Japan) was used as a stent for pancreatojejunostomy in all patients. Then, an end-to-side hepatojejunostomy was performed by a 1-layer anastomosis (5-0 PDS-II) 10 to 15 cm distal to the pancreatojejunostomy. Duodenojejunostomy in PpPD or gastrojejunostomy in PrPD was performed by a 2-layer anastomosis (4-0 PDS-II and 3-0 silk) via an antecolic route.[24] One 10-mm Penrose drain (a silicon, multitubular flat drain) was routinely placed anterior to the pancreatojejunostomy. This drain was connected to a closed drainage system. The drains were to be removed on postoperative day 4 in all patients if bile leakage and bacterial contamination were absent.[25] A 16-F nasogastric catheter was inserted and then removed from all patients on postoperative day 1.

No patient received radiotherapy preoperatively or postoperatively. All patients received an H_2-blocker (famotidine, Astellas Pharma, Inc, Tokyo, Japan) intravenously for 2 weeks postoperatively and prophylactic antibiotics intraoperatively and for 2 days postoperatively. Prophylactic octreotide or prokinetic agents such as erythromycin were not postoperatively administered to prevent pancreatic fistula or DGE.

Data Collection

Data were collected prospectively for all patients and included history, pathologic examination, perioperative clinical information, and complications. Before surgery and at 1, 3, and 6 months after surgery, nutritional status was assessed by serum nutritional parameters such as albumin, prealbumin, transferrin, and retinol-binding protein and body weights were measured. Upper gastrointestinal contrast study by gastrografin was performed on postoperative day 7. Time for the passage of gastrografin from the esophagogastric junction to gastrojejunostomy or duodenojejunostomy was measured.

The ^{13}C-acetate breath tests at 1, 3, and 6 months after surgery were performed to compare gastric emptying between PpPD and PrPD.[26] Patients ingested a liquid meal (200 kcal/200 mL, Racol, Ohtsuka Phama Co Ltd, Tokyo, Japan) labeled with 100-mg sodium ^{13}C-acetate (Cambridge Isotope Laboratories, Inc, Andover, Mass). Breath samples were collected in the collection bag before and at 5, 10, 15, 20, 30, 40, 50, 60, 75, and 90 minutes after ingestion of the test meal.[27] The $^{13}CO_2$ content was measured by infrared spectrophotometry (UBiT IR300, Otsuka Electronics Co Ltd, Osaka, Japan). Gastric emptying was evaluated on the basis of the time of peak $^{13}CO_2$ content.[28]

The QOL was recorded using Functional Assessment of Cancer Therapy–Gastric (FACT-Ga) questionnaire.[29] This questionnaire consists of the 27 items of the FACT-G, which provides a series of subscale scores for physical, social, emotional, and functional well-being and the newly validated 19-item scale, which assesses gastric cancer–specific domains of postoperative gastrointestinal symptoms

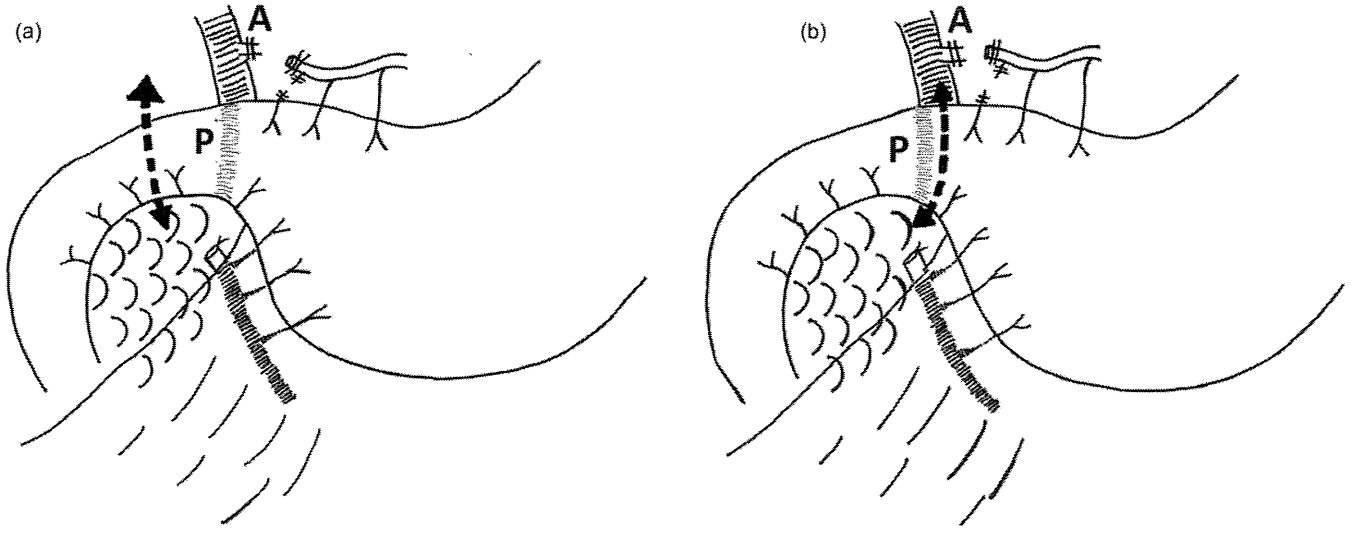

FIGURE 1. The right gastric artery (A) and vagal nerve were transected at the same levels in both PpPD and PrPD. The right gastric artery was dissected by the root, and the first pyloric branch was dissected along the lesser curvature of the stomach. The first pyloric branch of the right gastroepiploic artery was also dissected along the greater curvature of the stomach. The pyloric branch of the vagal nerve was dissected along with lymph nodes around the pylorus ring (P). (**a**), In PpPD, the proximal duodenum was divided 3 to 4 cm distal to the pylorus ring. (**b**), In PrPD, the stomach is divided just adjacent to the pylorus ring and more than 95% of the stomach can be preserved.

including dumping syndrome, gastric fullness, appetite loss, weight loss, diarrhea, and bile reflux gastritis. The patient's QOL by the FACT-Ga questionnaire was assessed at 1, 3, and 6 months after surgery.

Study End Points

The primary end point was the incidence of DGE. Delayed gastric emptying was defined according to a consensus definition and clinical grading of postoperative DGE proposed by the International Study Group of Pancreatic Surgery (ISGPS),[30] using the Web-based calculator (http://pancreasclub.com/calculator/) to improve the homogeneity of the definition.[16] Delayed gastric emptying is classified into 3 categories (grade A, B, or C) by ISGPS clinical criteria based on the clinical course and postoperative management such as reinsertion of a nasogastric catheter, the period of inability to tolerate a solid diet, presence or absence of vomiting, or use of prokinetics.[30]

Secondary end points were evaluation of QOL, nutritional status, postoperative complications except DGE, and mortality. *Pancreatic fistula* was defined by the ISGPF guideline: amylase level in fluid collection on postoperative day 3 that was more than 3 times the serum amylase level.[31] Pancreatic fistulae are classified into 3 categories (grades A, B, or C) by ISGPF clinical criteria. Intra-abdominal hemorrhage was defined by ISGPS.[32] Intra-abdominal hemorrhage is classified into 3 categories (grades A, B, or C) by ISGPS clinical criteria based on the clinical course. *Biliary fistulae* were defined as the presence of bile in drainage fluid that persisted by postoperative day 4. *Intra-abdominal abscess* was defined as intra-abdominal fluid collection with positive cultures identified by ultrasonography or computed tomography associated with persistent fever and elevations of white blood cell counts. Patients were discharged only when they fulfilled the criteria as follows: a return to preoperative activities of daily living, no deep-site infections, normal laboratory data, no drains, and the possibility for oral nutrition above the basal metabolism. *Mortality* was defined as death within 30 days after surgery.

Statistical Analysis

The study design to predict the number of patients necessary for statistical validity (2-sided) was based on the premise of improving DGE rate from 30% in PpPD to 10% in PrPD, with the α value set at .05 and the β value set at .2, yielding a power of 80%. We calculated that 65 patients were required in each arm of this study, for a total study population of 130 patients. Data were expressed as mean $\pm$ SD. Patient characteristics and perioperative and postoperative factors between the 2 groups were compared using χ^2 tests, the Fisher exact test, and the Mann-Whitney *U* test. *Statistical significance* was defined as $P < 0.05$.

RESULTS

Between October 2005 and March 2009 at WMUH, 139 patients with periampullary tumors were registered and 130 patients were enrolled in this study, with 64 patients randomized to PpPD and 66 to PrPD. Nine patients were excluded from this study before randomization because of the coexistence of hepatic cell carcinoma (n = 2), renal cell carcinoma (n = 1), severe cirrhosis (n = 1), hemodialysis (n = 1), psychological disorders (n = 1), and absence of informed consent (n = 3). A consort flow diagram of this RCT is shown in Figure 2.

Patient Characteristics

Table 1 shows the results of histologic analysis of the resected specimens, patient characteristics, preoperative status, and perioperative status. The 2 groups did not differ significantly in numbers with malignant (PpPD: n = 52; PrPD: n = 52) or benign tumors (PpPD:

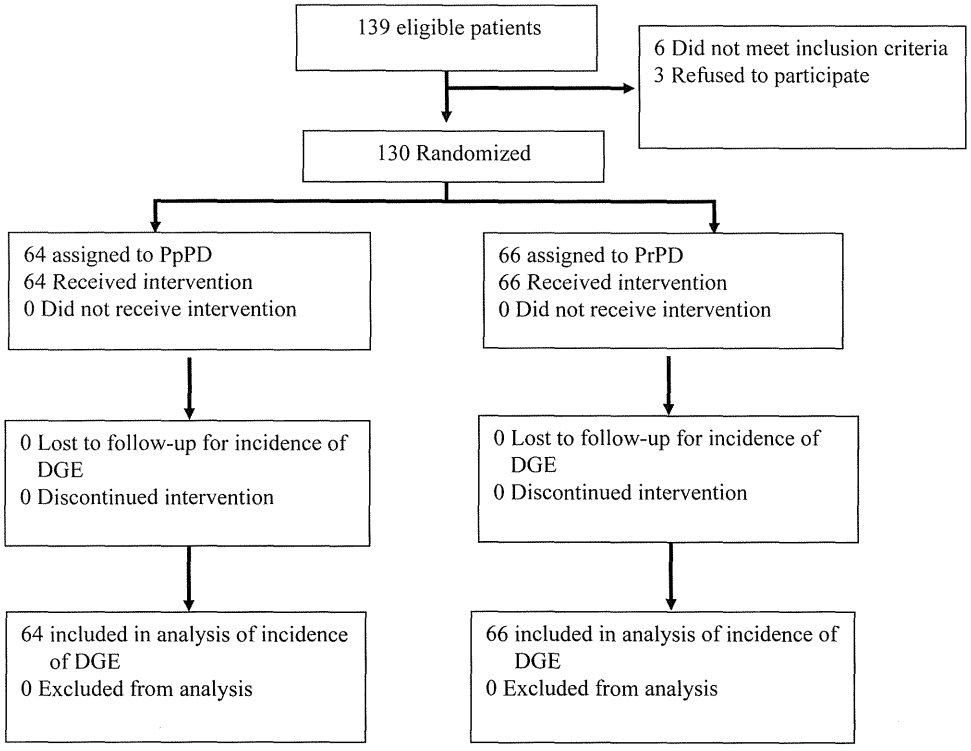

FIGURE 2. Study flow diagram. Nine patients were excluded from this study before randomization as indicated in the text.

TABLE 1. Characteristics of Enrolled Patients

	PpPD (n = 64)	PrPD (n = 66)	*P*
Age, yrs	68 ± 9	67 ± 9	0.5776
Gender (male/female)	33/31	38/28	0.6084
Diabetes (yes/no)	18/46	19/47	0.9999
Preoperative biliary drainage (yes/no)	34/33	26/40	0.2532
Diabetes (yes/no)	18/46	19/47	0.9999
Serum hemoglobin, g/dL*	13.0 ± 1.5	12.5 ± 1.3	0.2184
Serum creatinine, mg/dL†	0.68 ± 0.2	0.72 ± 0.2	0.1903
Serum total bilirubin, mg/dL‡	3.8 ± 4.0	4.0 ± 6.0	0.7965
Serum amylase, IU/L§	124 ± 134	111 ± 104	0.5232
Benign tumors/malignant tumors	12/52	14/52	0.8953
Pancreatic adenocarcinoma	17	23	
Bile duct carcinoma	18	15	
Ampullary adenocarcinoma	6	3	
Duodenal adenocarcinoma	0	1	
Intraductal papillary neoplasms	15	15	
Pancreatic endocrine tumor	1	2	
Tumor forming pancreatitis	3	5	
Other disease	4	2	
Operative time, min	342 ± 71	358 ± 84	0.2631
Intraoperative bleeding, mL	820 ± 987	902 ± 1075	0.6527
Red blood cell transfusion, units	1.1 ± 3.0	1.9 ± 5.0	0.2400
Lymph node dissection (D1/D2)	9/55	9/57	0.9999
Portal vein resection (yes/no)	5/59	10/56	0.3007

*Normal range of hemoglobin: 12–17.5 g/dL.
†Normal range of creatinine: 0.53–1.02 mg/dL.
‡Normal range of total bilirubin: 0.2–1.2 mg/dL.
§Normal range of amylase: 15–150 IU/L.

n = 12; PrPD: n = 14). Background data and perioperative status were similar in the 2 groups.

Incidence of DGE and Postoperative Course Associated With DGE

The overall incidence of DGE in this RCT was 10.8% (14 of the 130 patients); the overall incidence of DGE was 4.5% in PrPD and 17.2% in PpPD, a significant difference ($P = 0.0244$). Delayed gastric emptying was classified into 3 categories by ISGPS.[30] The proposed clinical grading of 11 patients with DGE in PpPD are grade A (n = 6), grade B (n = 5), and grade C (n = 0). In PrPD, 1 patient in each grade classification reported DGE. The 2 groups did not differ significantly in management of the nasogastric catheter, start of solid foods, and postoperative length of hospital stay (Table 2).

Time of passage from esophagogastric junction to gastrojejunostomy or duodenojejunostomy by postoperative upper gastrointestinal gastrografin series on postoperative day 7 was significantly delayed in PpPD compared with PrPD (27.2 ± 31.3 s versus 10.1 ± 9.0 s, $P < 0.0001$). The results of the time of peak $^{13}CO_2$ content are shown in Table 2. The time of peak $^{13}CO_2$ content at 1, 3, and 6 months after surgery in PpPD was significantly delayed compared with PrPD (34.3 ± 24.6 minutes versus 18.7 ± 11.8 minutes, 26.5 ± 21.1 minutes versus 17.3 ± 11.7 minutes, and 26.7 ± 18.8 minutes versus 17.4 ± 13.2 minutes, respectively). Thus, the gastric emptying of ^{13}C-acetate breath test or postoperative upper gastrointestinal gastrografin series was significantly delayed in patients in the PpPD group compared with those undergoing PrPD (Table 3).

TABLE 2. Delayed Gastric Emptying and Postoperative Course

	PpPD (n = 64)	PrPD (n = 66)	*P*
Delayed gastric emptying*	11 (17.2%)	3 (4.5%)	0.0244
Grade A	6 (9.4%)	1 (1.5%)	
Grade B	5 (7.8%)	1 (1.5%)	
Grade C	0 (0%)	1 (1.5%)	
Removal of nasogastric catheter, d	0.6 ± 0.9	0.6 ± 1.0	0.9410
Reinsertion of nasogastric catheter	8 (12.5%)	2 (3.0%)	0.0527
Start of solid diet, d	6.3 ± 3.7	5.6 ± 3.3	0.1138
Postoperative hospital stay, d	24.1 ± 14.8	24.3 ± 15.5	0.9305

*Delayed gastric emptying is defined according to the International Study Group of Pancreatic Surgeons.

TABLE 3. Results of Gastric Emptying Assessed by ^{13}C-Acetate Breath Test

	PpPD (n = 64)	PrPD (n = 66)	*P*
Postoperative upper gastrointestinal gastrografin series, s*	27.2 ± 31.3	10.1 ± 9.0	0.0001
^{13}C-acetate breath test, min†			
1 mo after surgery	34.0 ± 24.1	18.7 ± 29.7	<0.0001
3 mo after surgery	26.5 ± 21.1	17.3 ± 11.7	0.0136
6 mo after surgery	26.7 ± 18.8	17.4 ± 13.2	0.0197

*Time for the passage of gastrografin from esophagogastric junction to gastrojejunostomy or duodenojejunostomy was measured on postoperative day 7.
†Gastric emptying was evaluated by the time of peak $^{13}CO_2$ content in ^{13}C-acetate breath test at 1, 3, and 6 months after surgery.

Postoperative Complications

Table 4 shows the other postoperative complications in the PpPD and PrPD groups. The groups did not differ significantly in the incidence of other postoperative complications, specifically, clinically relevant pancreatic fistula, intra-abdominal abscess, and intra-abdominal hemorrhage. The overall rate of pancreatic fistula in this RCT was 29.2% (38 of 130 patients). Moreover, pancreatic fistula was classified into 3 categories by ISGPF[31]: grade A in 22 of the 130 patients (16.9%), grade B in 12 patients (9.2%), and grade C in 4 patients (3.1%). Ultrasonography-guided percutaneous drainage was required for intra-abdominal abscess in 14 (10.7%) of the 130 patients. Moreover, there was no significant difference between patients with and without pancreatic fistula concerning to the incidence of DGE (15.8% and 8.7% in patients with and without pancreatic fistula, respectively; $P = 0.3812$). All patients (n = 3) with intra-abdominal hemorrhage in this study were classified as grade B according to the criteria of ISGPS.[32] Although 1 patient in the PpPD group and 2 patients in PrPD group had intra-abdominal bleeding complicated by pancreatic fistula, complete hemostasis was achieved by interventional radiographic techniques. Reoperation rate in this study was 0.8% (1 of the 130 patients), and 1 patient underwent a reoperation requiring drainage on postoperative day (POD) 7 for pancreatic fistula. The postoperative course was uneventful and discharged on POD 40. The mortality rate in this study was 0.8% (1 of the 130 patients). One patient in the PrPD group died because of nonobstructive membrane ischemia.

TABLE 4. Postoperative Complications and Outcomes

	PpPD (n = 64)	PrPD (n = 66)	*P*
Pancreatic fistula*	19 (29.6%)	19 (28.8%)	0.9999
Grade A	11 (17.1%)	11 (16.7%)	
Grade B	7 (10.9%)	5 (7.6%)	
Grade C	1 (1.6%)	3 (4.5%)	
Intra-abdominal abscess	8 (12.5%)	6 (9.1%)	0.7309
Intra-abdominal hemorrhage	1 (1.6%)	2 (3.0%)	0.9999
Intraabdominal hemorrhage	1 (1.6%)	2 (3.0%)	0.9999
Grade A	0 (0%)	0 (0%)	
Grade B	1 (1.6%)	2 (3.0%)	
Grade C	0 (0%)	0 (0%)	
Wound infection	2 (3.1%)	2 (3.0%)	0.9999
Pulmonary complications	1 (1.6%)	2 (3.0%)	0.9999
NOMI	0 (0%)	1 (1.5%)	0.9999
Percutaneous drainage†	8 (12.5%)	6 (9.1%)	0.7309
Reoperation‡	0 (0%)	1 (1.5%)	0.9999
Mortality§	0 (0%)	1 (1.5%)	0.9999

*Pancreatic fistula is defined according to the International Study Group of Pancreatic Surgeons.

†Percutaneous drainage done as postoperative management of intra-abdominal abscess related to pancreatic fistula.

‡One patient underwent reoperation requiring drainage for pancreatic fistula.

§One patient died because of nonobstructive membrane ischemia (NOMI).

TABLE 5. Long-Term Outcomes Between PpPD and PrPD

	PpPD (n = 64)	PrPD (n = 66)	*P*
Quality of life			
Total FACT-Ga score, range 0–184			
1 mo after surgery	119.9 ± 24.3	120.4 ± 29.7	0.9205
3 mo after surgery	132.3 ± 21.3	125.4 ± 26.8	0.1630
6 mo after surgery	139.1 ± 22.9	139.6 ± 21.4	0.9140
FACT-Ga subscale, range 0–76			
1 mo after surgery	48.3 ± 12.3	49.2 ± 16.6	0.7479
3 mo after surgery	55.9 ± 10.2	53.9 ± 13.3	0.3935
6 mo after surgery	59.6 ± 11.0	60.1 ± 11.3	0.8137
Change of body weight, kg			
Before operation	54.9 ± 10	55.0 ± 9	0.9335
1 mo after surgery	50.0 ± 10	0.0 ± 8	0.8547
3 mo after surgery	49.8 ± 10	48.8 ± 8	0.5624
6 mo after surgery	50.9 ± 11	50.0 ± 8	0.4712
Endocrine function			
HbA_{1c},* %			
Before operation	5.8 ± 1.3	6.0 ± 1.7	0.4558
3 mo after surgery	5.6 ± 0.7	5.6 ± 0.8	0.9596
6 mo after surgery	5.7 ± 1.0	5.7 ± 1.2	0.8534
New-onset or worsening diabetes†	3/64 (4.7%)	2/66 (3.0%)	0.6777
New diabetes	2	1	
Worsening diabetes	1	1	

*Normal range of HbA_{1c}: 3.8–5.1 g/dL.

†*New-onset diabetes* is defined as diabetes requiring new medical treatment such as diet treatment, oral drug, or insulin. *Worsening diabetes* is defined as diabetes requiring a modification of the medical treatment for deterioration of previously diagnosed diabetes.

Comparison of QOL, Nutritional Status, and Body Weight Change Between PpPD and PrPD

The overall QOL scores from the FACT-Ga scales are presented in Table 5. The highest possible scores for the physical, social, emotional, and functional subscales in FACT-G are 28, 28, 24, and 28, respectively. The highest possible score for the 19-item FACT-Ga subscale is 76. The highest possible score of total FACT-Ga score by combining total FACT-G score and FACT-Ga subscale is 184. No significant differences were found in the results of any subscale score or the total FACT-Ga scores at 1, 3, and 6 months after surgery between PpPD and PrPD.

Moreover, the patients who underwent PpPD and PrPD did not differ significantly in endocrine function or body weight change before surgery and at 1, 3, and 6 months postoperatively (Table 5).

Among serum nutritional parameters as assessment of nutritional status, rapid turnover proteins, such as albumin, prealbumin, transferrin, and retinol-binding protein, were decreased at 1 month after surgery. The levels were gradually restored thereafter and recovered to baseline or higher than the preoperative levels at 6 months after surgery. The changes in those parameters were similar in the 2 groups (Table 6).

DISCUSSION

The reported overall incidence of DGE according to the new definitions from ISGPS is 33% to 47%.[15,16,32] In previous studies, the pathogenesis of DGE after PpPD has been thought to include several factors, such as (1) antroduodenal ischemia,[20,33] (2) gastric atony caused by vagotomy,[34] (3) pylorospasm,[17–19] (4) absence of gastrointestinal hormone,[35] (5) gastric dysrhythmia secondary to other complications such as pancreatic fistula,[12,14,36–39] and (6) antroduodenal congestion.[21] Operative techniques using antecolic reconstruction for duodenojejunostomy[24] and postoperative management using erythromycin[20,35] were reported to reduce the incidence of DGE. However, the relatively high incidence of DGE after PpPD remains unsolved and we should consider ways to improve the surgical technique to decrease the incidence of DGE.

None of the 139 eligible patients in this study had lymph nodes metastasis of the peripylorus region. However, infrapyloric lymph nodes metastasis in pancreatic head carcinoma was reported to be 12%.[40] Therefore, the sampling or dissection of the peripylorus lymph nodes should be needed in patients with pancreatic head carcinoma. In the present study, we hypothesized that preservation of the pylorus ring is a risk factor for DGE and assessed whether resection of the pylorus ring with preservation of nearly the entire stomach (designated as PrPD) would significantly reduce the incidence of DGE compared with that in conventional PpPD. The results confirmed our hypotheses with the DGE rate of 17.2% in PpPD compared with that of 4.5% in PrPD ($P = 0.0244$). This is the first RCT to clarify that PrPD reduces the incidence of DGE compared with PpPD. If such reduced incidence of DGE is achieved by PrPD, one would expect a shorter hospital stay in the PrPD group. However, postoperative hospital stay in both groups may be longer than that observed in the Western countries. The Japanese health care system is different from the Western countries. Therefore, comparing lengths of postoperative hospital stay is difficult between Japan and the Western countries. Several studies proposed that gastric dysrhythmia secondary to other abdominal complications, such as pancreatic fistula or intra-abdominal abscess, induced the incidence of DGE.[12,14,36–39] In the present study, we found no significant differences between PpPD and PrPD in the incidence of clinically relevant pancreatic fistula or intra-abdominal abscess. Therefore, other postoperative complications had no bias or influence on the incidence of DGE in this study evaluating the 2 procedures. Many pancreatic surgeons believe that DGE after PD is

TABLE 6. Nutritional Status Between PpPD and PrPD

	PpPD (n = 64)	PrPD (n = 66)	*P*
Albumin,* g/dL			
Before operation	4.1 ± 0.5	4.0 ± 0.5	0.6493
1 mo after surgery	3.6 ± 0.6	3.7 ± 0.5	0.5425
3 mo after surgery	3.9 ± 0.6	3.8 ± 0.6	0.2810
6 mo after surgery	4.0 ± 0.4†	3.9 ± 0.4†	0.4153
Prealbumin,‡ g/dL			
Before operation	22.2 ± 7.1	21.0 ± 6.3	0.3192
1 mo after surgery	15.4 ± 5.4	15.2 ± 4.8	0.7877
3 mo after surgery	19.0 ± 5.9	17.4 ± 4.6	0.1147
6 mo after surgery	21.0 ± 5.0†	19.4 ± 5.7†	0.0944
Transferrin,§ mg/dL			
Before operation	233 ± 49	233 ± 42	0.9892
1 mo after surgery	197 ± 47	197 ± 47	0.9694
3 mo after surgery	225 ± 52	213 ± 59	0.2532
6 mo after surgery	252 ± 52†	232 ± 57†	0.0587
Retinol-binding protein, • mg/dL			
Before operation	3.7 ± 1.4	3.4 ± 1.2	0.2089
1 mo after surgery	2.4 ± 0.9	2.3 ± 0.9	0.5518
3 mo after surgery	2.9 ± 1.0	2.6 ± 1.0	1003
6 mo after surgery	3.1 ± 1.1†	3.0 ± 1.2†	6579

*Normal range of albumin: 3.8–5.1 g/dL.
†The level at 6 months after surgery recovered to the baseline or higher than the preoperative level.
‡Normal range of prealbumin: 22–40 mg/dL.
§Normal range of transferrin: 200–400 mg/dL.
•Normal range of retinol-binding protein: 2.4–7 mg/dL.

caused by local and systemic septic complications. This study again demonstrates that there are complication-unrelated mechanisms for DGE.

As for prophylactic management of pylorospasm due to denervation after PpPD, 2 reports described the operative technique including the mechanical dilatation of the pylorus ring and pyloromyotomy.[18,19] It has been proposed that the addition of pyloric dilatation in PpPD reduces the incidence of DGE from 26% to 6.5% ($P < 0.05$) compared with conventional that in PpPD.[18] On the other hand, the addition of pyloromyotomy in PpPD reduces the incidence of DGE from 21% to 2% ($P < 0.01$) compared with that in conventional PpPD.[19] However, these 2 studies were not RCTs. To avoid bias issues, RCTs should be performed to determine the better surgical procedure.

The ^{13}C-acetate breath test is a simple and excellent indirect test for gastric emptying.[26] In particular, the time of peak $^{13}CO_2$ content has been reported to be a more useful marker reflecting gastric emptying.[28] To our knowledge, no reports have evaluated gastric emptying by the ^{13}C-acetate breath test in patients with pancreatic head resection. In this study, gastric emptying assessed by the ^{13}C-acetate breath test at 1, 3, and 6 months after surgery was significantly delayed in patients undergoing PpPD compared with that in those undergoing PrPD. This result of the ^{13}C-acetate breath test supported the hypothesis that the incidence of DGE was significantly lower in PrPD (4.5%) than in PpPD (17.1%). On the other hand, rapid gastric emptying in the ^{13}C-acetate breath test seems to reflect dumping syndrome after gastrectomy. However, only 1 of 66 patients (1.5%) in the PrPD group had dumping syndrome, and no patient undergoing PpPD had this complication.

Pylorus-preserving pancreatoduodenectomy has been reported to reduce syndromes occurring after gastrectomy, including dumping syndrome, diarrhea, and poor recovery of body weight and to afford patients a better nutritional status compared with that in PD with antrectomy.[8–12] Pylorus-resecting pancreatoduodenectomy may lead to gastrectomy syndromes because of resecting the pylorus ring, as done in PD with antrectomy. Moreover, no reports have evaluated QOL for syndromes after gastrectomy or gastric emptying function between patients with preservation and resection of the pylorus ring in PD. The gastric cancer–specific FACT-Ga questionnaire, which consists of the 27 items from the FACT-G and 19 gastric cancer–specific items, was reported to reflect postgastrectomy syndromes.[29] The incidence of DGE greatly influences postgastrectomy syndrome or postoperative gastric emptying function. We believe that FACT-Ga is the best QOL questionnaire to evaluate the differences of QOL in patients with or without DGE. Therefore, FACT-Ga questionnaire was chosen in this RCT to compare PpPD and PrPD regarding postgastrectomy syndromes or gastric emptying function. In this study, no significant differences occurred in postgastrectomy syndromes or sensation of gastric fullness between PpPD and PrPD. More than 95% of the stomach is preserved in PrPD, and the stomach pooling ability is preserved in PrPD in the same way as in PpPD, although the pylorus ring was resected. However, the next step is to clarify whether PrPD is a better surgical procedure compared with conventional PD with antrectomy.

In conclusion, this study suggested that PrPD can lead to a significant reduction in the incidence of DGE compared with conventional PpPD. The patients enrolled in this study will be followed carefully in terms of nutritional status and QOL for 1 year and 2 years postoperatively and evaluated for the better procedure.

REFERENCES

1. Traverso LW, Longmire WJ. Preservation of the pylorus in pancreaticoduodenectomy. *Surg Gynecol Obstet*. 1978;146:959–962.
2. Lin PW, Lin YJ. Prospective randomized comparison between pylorus preserving and standard pancreaticoduodenectomy. *Br J Surg*. 1999;86:603–607.
3. Seiler CA, Wagner M, Sadowski C, et al. Randomized prospective trial of pylorus-preserving vs classic duodenopancreatectomy (Whipple procedure): initial clinical results. *J Gastrointest Surg*. 2000;4:443–452.
4. Tran KTC, Smeenk HG, van Eijck CHJ, et al. Pylorus preserving pancreaticoduodenectomy versus standard Whipple procedure. A prospective, randomized, multicenter analysis of 170 patients with pancreatic and periampullary tumors. *Ann Surg*. 2004;240:738–745.
5. Seiler CA, Wagner M, Bachmann CA, et al. Randomized clinical trial of pylorus-preserving duodenopancreatectomy versus classical Whipple resection—long term results. *Br J Surg*. 2005;92:547–556.
6. Lin PW, Shan YS, Lin YJ, et al. Pancreaticoduodenectomy for pancreatic head cancer: PPPD versus Whipple procedure. *Hepatogastroenterology*. 2005;52:1601–1604.
7. Diener MK, Knaebel HP, Heukaufer C, et al. A systematic review and meta-analysis of pylorus-preserving versus classical pancreaticoduodenectomy for surgical treatment of periampullary and pancreatic carcinoma. *Ann Surg*. 2007;245:187–200.
8. Traverso LW, Longmire WJ. Preservation of the pylorus in pancreaticoduodenectomy: a follow-up evaluation. *Ann Surg*. 1980;192:306–310.
9. Jimenez RE, Femandez-del Castillo C, Rattner DW, et al. Outcome of pancreaticoduodenectomy with pylorus preservation or with antrectomy in the treatment of chronic pancreatitis. *Ann Surg*. 2000;231:293–300.
10. Brasssch JW, Deziel DJ, Rossi RL, et al. Pyloric and gastric preserving pancreatic resection. Experience with 87 patients. *Ann Surg*. 1986;204:411–418.
11. Hunt DR, McLean R. Pylorus-preserving pancreatectomy: functional results. *Br J Surg*. 1989;76:173–176.
12. van Berge Henegouwewn MI, van Gulik TM, De Wit LT, et al. Delayed gastric emptying after standard pancreaticoduodenectomy versus pylorus-preserving pancreaticoduodenectomy: an analysis of 200 consecutive patients. *J Am Coll Surg*. 1997;185:373–379.

13. Yeo CJ, Cameron JL, Sohn TA, et al. Six hundred fifty consecutive pancreaticoduodenectomy in the 1990s: pathology, complications, and outcomes. *Ann Surg*. 1997;226:248–257.
14. Horstmann O, Markus PM, Ghadimi MB, et al. Pylorus preservation has no impact on delayed gastric emptying after pancreatic head resection. *Pancreas*. 2004;28:69–74.
15. Akizuki E, Kimura Y, Nobuoka T, et al. Reconsideration of postoperative oral intake tolerance after pancreaticoduodenectomy—prospective consecutive analysis of delayed gastric emptying according to the ISGPS definition and the amount of dietary intake. *Ann Surg*. 2009;249:986–994.
16. Hashimoto Y, Traverso LW. Incidence of pancreatic anastomotic failure and delayed gastric emptying after pancreatoduodenectomy in 507 consecutive patients: use of a web-based calculator to improve homogeneity of definition [published online ahead of print December 15, 2009]. *Surgery*. 2010;147:503–515.
17. Gauvin JM, Sarmiento JM, Sarr MG. pylorus-preserving pancreaticoduodenectomy with complete preservation of the pyloroduodenal blood supply and innervation. *Arch Surg*. 2003;138:1261–1263.
18. Fischer CP, Hong JC. Method of pyloric reconstruction and impact upon delayed gastric emptying and hospital stay after pylorus-preserving pancreaticoduodenectomy. *J Gastrointest Surg*. 2006;10:215–219.
19. Kim DK, Hindenburg AA, Sharma SK, et al. Is pylorospasm a cause of delayed gastric emptying after pylorus-preserving pancreaticoduodenectomy? *Ann Surg Oncol* 2005;12:222–227.
20. Ohwada S, Satoh Y, Kawate S, et al. Low-dose erythromycin reduces delayed gastric emptying and improves gastric motility after Billroth I pylorus-preserving pancreaticoduodenectomy. *Ann Surg*. 2001;234:668–674.
21. Kurosaki I, Hatakeyama K. Preservation of the left gastric vein in delayed gastric emptying after pylorus-preserving pancreaticoduodenectomy. *J Gastrointest Surg*. 2005;9:846–852.
22. Tani M, Kawai M, Terasawa H, et al. Complication with reconstruction procedure in pylorus-preserving pancreaticojejunostomy. *World J Surg*. 2005;29:881–884.
23. Tani M, Onishi H, Kinosita H, et al. The evaluation of duct-to mucosal pancreaticojejunostomy in pancreaticoduodenostomy. *World J Surg*. 2005;29:76–79.
24. Tani M, Terasawa H, Kawai M, et al. Improvement of delayed gastric emptying in pylorus-preserving pancreaticoduodenectomy: results of a prospective, randomized, controlled trial. *Ann Surg* 2006;243:316–320.
25. Kawai M, Tani M, Terasawa H, et al. Early removal of prophylactic drains reduces the risk of intra-abdominal infections in patients with pancreatic head resection: prospective study for consecutive 104 patients. *Ann Surg*. 2006;244:1–7.
26. Braden B, Adams S, Duan LP, et al. The [13C]acetate breath test accurately reflects gastric emptying of liquids in both liquid and semisolid test meals. *Gastroenterology*. 1995;108:1048–1055.
27. Nakata K, Aoyama N, Nakagawa M, et al. The present and the future in gastric emptying study assessed by ^{13}C-acetate breath test—with special reference to the standardization of the method [in Japanese]. *J Smooth Muscle Res*. 2002;6:J75–J91.
28. Urita Y, Hike K, Torii N, et al. Efficacy of lactulose plus ^{13}C-acetate breath test in the diagnosis of gastrointestinal motility disorders. *J Gastroenterol*. 2002;37:442–448.
29. Eremenco SL, Cashy J, Webster K, et al. FACT-Gastric: a new international measure of QOL in gastric cancer. *ASCO Proc*. 2004;23:755. Abstract 8123.
30. Wente MN, Bassi C, Dervenis C, et al. Delayed gastric emptying (DGE) after pancreatic surgery: a suggested definition by the International Study Group of Pancreatic Surgery (ISGPS). *Surgery*. 2007;142:761–768.
31. Bassi C, Dervenis C, Butturini G, et al. Postoperative pancreatic fistula: an international study group (ISGPF) definition. *Surgery*. 2005;138:8–13.
32. Wente MN, Veit JA, Bassi C, et al. Postpancreatectomy hemorrhage (PPH)—an International Study Group of Pancreatic Surgery (ISGPS) definition. *Surgery*. 2007:142,20–25.
33. Park JS, Hwang HK, Kim JK, et al. Clinical validation and risk factors for delayed gastric emptying based on the International Study Group of Pancreatic Surgery (ISGPS) Classification. *Surgery*. 2009;146:882–887.
34. Itani KM, Coleman RE, Meyers WC, et al. Pylorus-preserving pancreaticoduodenectomy. A clinical and physiologic appraisal. *Ann Surg*. 1986;204:655–664.
35. Kobayasi I, Miyachi M, Kanai M, et al. Different gastric emptying of solid and liquid meals after pylorus-preserving pancreaticoduodenectomy. *Br J Surg*. 1998;85:927–930.
36. Yeo CJ, Barry MK, Sauter PK, et al. Erythromycin accelerates gastric emptying following pancreaticoduodenectomy: a prospective, randomized placebo-controlled trial. *Ann Surg*. 1993;218:229–238.
37. Raty S, Sand J, Lantto E, et al. Postoperative acute pancreatitis as a major determinant of postoperative delayed gastric emptying after pancreaticoduodenectomy. *J Gastrointest Surg*. 2006;10:1131–1139.
38. Riediger H, Makowiec F, Schareck WD, et al. Delayed gastric emptying after pylorus-preserving pancreaticoduodenectomy is strongly related to other postoperative complications. *J Gastrointest Surg*. 2003;7:758–765.
39. Miedema BW, Sarr MG, van Heerden JA, et al. Complications following pancreaticoduodenectomy: current management. Arch Surg. 1992;127:945–949.
40. Sakai M, Nakao A, Kaneko T, et al. Para-aortic lymph node metastasis in carcinoma of the head of the pancreas. *Surgery*. 2005; 137:606–611.

uicc
global cancer control

IJC
International Journal of Cancer

Overexpression of LSD1 contributes to human carcinogenesis through chromatin regulation in various cancers

Shinya Hayami[1,2], John D. Kelly[3], Hyun-Soo Cho[1], Masanori Yoshimatsu[1], Motoko Unoki[4], Tatsuhiko Tsunoda[5], Helen I. Field[6], David E. Neal[7], Hiroki Yamaue[2], Bruce A.J. Ponder[7], Yusuke Nakamura[1] and Ryuji Hamamoto[1,7]

[1] Laboratory of Molecular Medicine, Human Genome Center, Institute of Medical Science, The University of Tokyo, Minato-ku, Tokyo, Japan
[2] Second Department of Surgery, School of Medicine, Wakayama Medical University, Wakayama, Japan
[3] Division of Surgery and Interventional Science, UCL Medical School, University College London, London, United Kingdom
[4] Laboratory for Biomarker Development, RIKEN, Minato-ku, Tokyo, Japan
[5] Laboratory for Medical Informatics, RIKEN, Tsurumi-ku, Yokohama, Kanagawa, Japan
[6] Department of Oncology, Strangeways Research Laboratory, University of Cambridge, Worts Causeway, Cambridge, United Kingdom
[7] Department of Oncology, Cancer Research UK Cambridge Research Institute, University of Cambridge, Robinson Way, Cambridge, United Kingdom

A number of histone demethylases have been identified and biochemically characterized, but the pathological roles of their dysfunction in human disease like cancer have not been well understood. Here, we demonstrate important roles of lysine-specific demethylase 1 (LSD1) in human carcinogenesis. Expression levels of *LSD1* are significantly elevated in human bladder carcinomas compared with nonneoplastic bladder tissues ($p < 0.0001$). cDNA microarray analysis also revealed its transactivation in lung and colorectal carcinomas. LSD1-specific small interfering RNAs significantly knocked down its expression and resulted in suppression of proliferation of various bladder and lung cancer cell lines. Concordantly, introduction of exogenous LSD1 expression promoted cell cycle progression of human embryonic kidney fibroblast cells. Expression profile analysis showed that LSD1 could affect the expression of genes involved in various chromatin-modifying pathways such as chromatin remodeling at centromere, centromeric heterochromatin formation and chromatin assembly, indicating its essential roles in carcinogenesis through chromatin modification.

Histone methylation plays important dynamic roles in regulating chromatin structure. Precise conformational regulation of chromatins is crucial for normal cellular processes such as DNA replication, DNA repair, chromosome recombination and mRNA transcription. Although histone methylation was considered to be a static modification until recently, the discovery of lysine-specific demethylase 1 (LSD1), which specifically demethylates mono- and dimethylated histone H3 at lysine 4 (H3-K4), indicated that the histone methylation was reversible.[1] Subsequently, a JmjC domain-containing protein was identified to possess histone demethylase activity, and the JmjC domain was shown to be a demethylase signature motif.[2] JmjC domain-containing enzymes catalyze the removal of methyl groups using a hydroxylation reaction, requiring iron and α-ketoglutarate cofactors. Several additional proteins were identified as histone lysine demethylases on the basis of the presence of the JmjC motif.[3–9] Although information of histone demethylases in their physiological function has been accumulated, their involvement in human disease remains unclear.

We previously reported that SMYD3, a histone methyltransferase, stimulates cell proliferation through its methyltransferase activity and plays a crucial role in human carcinogenesis.[10–14] Dysfunction of histone methylation was also shown to contribute to human carcinogenesis,[15–17] but the relationship between abnormal histone demethylation and human carcinogenesis is still largely unclear. To find demethylases involved in human carcinogenesis, we screened a number of histone demethylases in clinical tissues by expression profile analysis and found transactivation of LSD1 in various types of cancer.

LSD1, also known as AOF2, is a histone demethylase that does not belong to the JmjC family, catalyzing the demethylation of histone H3-K4 and K9. LSD1 is composed of several domains, including a SWIRM domain, a conserved motif shared by many chromatin regulatory complexes, an amine oxidase domain and a Tower domain found in BRCA2.[18–20] LSD1 cooperates with CoREST,[21–23] CtBP[24] corepressor complex and demethylates histone H3-K4 through this interaction. LSD1 also demethylates histone H3-K9 and regulates

Key words: LSD1, histone demethylase, epigenetics, bladder cancer, chromatin modification
Additional Supporting Information may be found in the online version of this article
Grant sponsors: NIHR, Cambridge Biomedical Research Centre
DOI: 10.1002/ijc.25349
History: Received 10 Sep 2009; Accepted 23 Mar 2010; Online 23 Mar 2010
Correspondence to: Yusuke Nakamura, Laboratory of Molecular Medicine, Human Genome Center, Institute of Medical Science, The University of Tokyo, 4-6-1 Shirokanedai, Minato-ku, Tokyo 108-8639, Japan, Fax: +81-3-5449-5372, E-mail: yusuke@ims.u-tokyo.ac.jp

transcription in the presence of the human androgen receptor.[25–27] In addition to histone proteins, LSD1 was reported to demethylate p53 lysine 370 and repress p53-mediated transcriptional upregulation as well as its apoptosis-promoting action.[28–30] LSD1 was also shown to form a stable complex with RB and decrease H3-K4 methylation level, causing reduction of transcription from the Epstein Barr Virus-C promoter.[31] Here, we demonstrate possible involvement of LSD1 in human carcinogenesis and imply LSD1 as a candidate therapeutic target for various types of cancer.

Material and Methods

Tissue samples and RNA preparation

One hundred and twenty-one surgical specimens of primary urothelial carcinoma were collected, either at cystectomy or transurethral resection of bladder tumor, and snap frozen in liquid nitrogen. Twenty-six specimens of normal bladder urothelial tissue were collected from areas of macroscopically normal bladder urothelium in patients with no evidence of malignancy. Five sequential sections of 7-μm thickness were cut from each tissue and stained using Histogene™ staining solution (Arcturus, CA) following the manufacturer's protocol and assessed for cellularity and tumor grade by an independent consultant urohistopathologist. Slides were then transferred for microdissection using PixCell™ II laser capture microscope (Arcturus). This technique uses a low-power infrared laser to melt a thermoplastic film over the cells of interest, to which the cells become attached. Additionally, the sections were graded according to the degree of inflammatory cell infiltration (low, moderate and severe). Samples showing significant inflammatory cell infiltration were excluded.[32]

Approximately 10,000 cells were microdissected from both stromal and epithelial/tumor compartments in each tissue. RNA was extracted using an RNeasy Micro Kit (QIAGEN, Crawley, UK). Areas of tumor or stroma containing significant inflammatory cell infiltration were avoided to prevent contamination.[32] Total RNA was reverse transcribed, and qRT-PCR performed as below. Given the low yield of RNA from such small samples, NanoDrop™ quantification was not performed, but correction for the endogenous 18S CT value was used as an accurate measure of the amount of intact starting RNA. To validate the accuracy of microdissection, primers and probes for Vimentin and Uroplakin were sourced, and qRT-PCR performed according to the manufacturer's instructions (Assays on demand, Applied Biosystems, Warrington, UK). Vimentin is primarily expressed in mesenchymally derived cells and was used as a stromal marker. Uroplakin is a marker of urothelial differentiation and is preserved in up to 90% of epithelially derived tumors.[33] Use of tissues for this study was approved by Cambridge shire Local Research Ethics Committee (Ref 03/018).

Cell culture

All cell lines were grown in monolayers in appropriate media: Dulbecco's modified Eagle's medium for EJ28 bladder cancer cells and RERF-LC-AI non-small cell lung cancer cells; Eagle's minimal essential medium for 253J, 253J-BV, HT1197, HT1376, J82, SCaBER, UMUC3 bladder cancer cells and SBC5 small cell lung cancer cells; Leibovitz's L-15 for SW780 cells; McCoy's 5A medium for RT4 and T24 bladder cancer cells; RPMI1640 medium for 5637 bladder cancer cells and A549, H2170 and LC319 non-small cell lung cancer cells supplemented with 10% fetal bovine serum and 1% antibiotic/antimycotic solution (Sigma). All cells were maintained at 37°C in humid air with 5% CO_2 condition (5637, 253J, 253J-BV, EJ28, HT1197, HT1376, J82, RT4, SCaBER, T24, UMUC3, A549, H2170, LC319, RERF-LC-AI and SBC5) or without CO_2 (SW780). Cells were transfected with FuGENE6™ (Roche Applied Science, Basel, Switzerland) according to the manufacturer's protocols.

Expression profiling in cancers using cDNA microarrays

We established a genome-wide cDNA microarray with 36,864 cDNAs or ESTs selected from the UniGene database of the National Center for Biotechnology Information. This microarray system was constructed essentially as described previously.[34–36] Briefly, the cDNAs were amplified by RT-PCR using poly $(A)^+$ RNAs isolated from various human organs as templates; the lengths of the amplicons ranged from 200 to 1,100 bp, without any repetitive or poly (A) sequences. Many types of tumors and corresponding nonneoplastic tissues were prepared in 8-μm sections, as described previously.[35] A total of 30,000–40,000 cancer or noncancerous cells were collected selectively using the EZ cut system (SL Microtest GmbH, Germany) according to the manufacturer's protocol. Extraction of total RNA, T7-based amplification and labeling of probes were performed as described previously.[35] A total of 2.5-μg aliquots of twice-amplified RNA from each cancerous and noncancerous tissue were then labeled, respectively, with Cy3-dCTP or Cy5-dCTP. Detailed expression profiling data of bladder, lung and colorectal cancers in this study were based on the data reported previously by Dr. Takefumi Kikuchi, Dr. Yu-Min Lin and Dr. Ryo Takata, respectively.[34,37,38]

Quantitative real-time PCR

As described above, we obtained 121 bladder cancer and normal 26 bladder tissues in Cambridge Addenbrooke's Hospital. For quantitative RT-PCR reactions, specific primers for all human *GAPDH* (housekeeping gene), *SDH* (housekeeping gene) and *LSD1* were designed (primer sequences in Supporting Information Table 1). PCR reactions were performed using the ABI prism 7700 Sequence Detection System (Applied Biosystems, Warrington, UK) following the manufacturer's protocol. Fifty percent of SYBR Green universal PCR Master Mix without UNG (Applied Biosystems, Warrington, UK), 50 nM each of the forward and reverse primers and 2 μl of reverse transcriptional cDNA were applied. Amplification conditions were first at 95°C for 5 min and then 45 cycles, each at 95°C for 10 sec, at 55°C

for 1 min and at 72°C for 10 sec. After this, we treated samples at 95°C for 15 sec, then at 65°C for 1 min to draw the melting curve and then cooled to 50°C for 10 sec. Reaction conditions for target gene amplification were as described above, and the equivalent of 5 ng of reverse transcribed RNA was used in each reaction. mRNA levels were normalized to *GAPDH* and *SDH* expression.

To determine relative RNA levels within the samples, standard curves for the PCR reactions were prepared from a series of 2-fold dilutions of cDNA covering the range 2–0.625 ng of RNA for the 18S reaction and 20–0.5 ng of RNA for all target genes. The ABI prism 7700 measured changes in fluorescence levels throughout the 45 cycles PCR reaction and generated a cycle threshold (C_t) value for each sample correlating to the point at which amplification entered the exponential phase. This value was used as an indicator of the amount of starting template; hence, a lower C_t values indicated a higher amount of initial intact cDNA.

Transfection with small interfering RNAs

The small interfering RNA (siRNA) oligonucleotide duplexes were purchased from SIGMA Genosys for targeting the human LSD1 transcript. siEGFP and siNegative control, which is a mixture of 3 different oligonucleotide duplexes, were used as control siRNAs. The siRNA sequences are described in Supporting Information Table 2. siRNA duplexes (100 nM final concentration) were transfected to bladder and lung cancer cell lines with Lipofectamine 2000 (Invitrogen). After 72 hr, cell viability was examined using cell counting kit 8 (DOJINDO).

Construction of stable cell lines, constitutively expressing LSD1

We prepared V5-tagged LSD1 expression vectors (pcDNA5/FRT/V5-His-LSD1) and transfected those into Flp-In T-REx 293 cells (Invitrogen), which contain a Flp recombination target (FRT) site in its genome to express LSD1 conditionally and stably. V5-tagged chloramphenicol acetyltransferase (CAT) expression vectors (pcDNA5/FRT/V5-His-CAT) were used as a negative control for the experiments. LSD1 expression at the protein level was evaluated by Western blot and immunocytochemistry (Supporting Information Fig. 1).

Flow cytometry assays for cell cycle analysis of stable cell lines

We prepared 3 stable T-REx 293 cell lines: mock-transfected with unmodified vector (pcDNA5/FRT/V5-His), vector expressing CAT (pcDNA5/FRT/V5-His-CAT) and vector expressing LSD1 (pcDNA5/FRT/V5-His-LSD1). Then, we collected the cells after trypsin treatment, washed twice with 1,000 μl of assay buffer and centrifuged for 5 min at 5,000 rpm. Cells were resuspended in 200 μl of assay buffer. A total of 1,000 μl of fixative buffer was added, and the samples incubated at room temperature for 1 hr. Finally, we added the propidium iodide reagent and analyzed cell cycle profiles by flow cytometry (LSR II, BD Biosciences). The proportion of each cell division was calculated and analyzed using Student's *t*-test for significance.

Coupled cell cycle and cell proliferation assay

A 5′-bromo-2′-deoxyuridine (BrdU) flow kit (BD Pharmingen, San Diego, CA) was used to determine the cell cycle kinetics and to measure the incorporation of BrdU into DNA of proliferating cells. The assay was performed according to the manufacturer's protocol. Briefly, cells (2×10^5 per well) were seeded overnight in 6-well tissue culture plates and treated with an optimized concentration of siRNAs in medium containing 10% FBS for 72 hr, followed by addition of 10 μM BrdU and incubations continued for an additional 30 min. Both floating and adherent cells were pooled from triplicates wells per treatment point, fixed in a solution containing paraformaldehyde and the detergent saponin and incubated for 1 hr with DNase at 37°C (30 μg per sample). FITC-conjugated anti-BrdU antibody (1:50 dilution in wash buffer; BD Pharmingen, San Diego, CA) was added and incubation continued for 20 min at room temperature. Cells were washed in wash buffer, and total DNA was stained with 7-amino-actinomycin D (7-AAD; 20 μL per sample), followed by flow cytometric analysis using FACScan (Beckman Coulter) and total DNA content (7-AAD) was determined by CXP Analysis Software Ver. 2.2 (Beckman Coulter).

Imunohistochemical staining

Sections of human bladder cancer were stained by Vectastain® ABC Kit (Vector Laboratories, CA). Briefly, endogenous peroxidase activity of xylene-deparaffinized and dehydrated sections was inhibited by treatment with 0.3% H_2O_2/methanol. Nonspecific binding was blocked by incubating sections with 3% BSA in a humidified chamber for 30 min at ambient temperature, then a 1:100 dilution of rabbit polyclonal anti-LSD1 antibody (ab17721-100, abcam, Tokyo, Japan) overnight at 4°C. Sections were washed twice with PBS (−), incubated with 5 μg/μl goat anti-mouse biotinylated IgG in PBS containing 1% BSA for 30 min at ambient temperature and then incubated with ABC reagent for 30 min. Immunostaining was visualized using 3,3′-diaminobenzidine. Slides were dehydrated through graded alcohol to xylene washing and mounted on cover slips.

Microarray hybridization and statistical analysis for the clarification of downstream genes

Purified total RNA was labeled and hybridized onto Affymetrix Human GeneChip U133 Plus 2.0 oligonucleotide arrays (Affymetrix, Santa Clara, CA) according to the manufacturer's instructions. Probe signal intensities were normalized by RMA and Quantile normalization methods (using R and Bioconductor). Next, signal intensity fluctuation due to inter-experimental variation was estimated. Each experiment was replicated (1 and 2), and the standard deviation (stdev) of $\log_2(\text{intensity}_2/\text{intensity}_1)$ was calculated for each of a set of

Table 1. Clinicopathologic characterstics and [*LSD1*] expression

Tissue	Sample name	*LSD1* expression	Stage	Grade
Bladder tumor	BT2	10.075	T4	G3
	BT5	7.506	Ta	Uk
	BT6	4.300	Ta	G2
	BT8	5.182	Ta	G2
	BT9	16.928	Ta	G2
	BT10	6.380	T2	G3
	BT11	6.918	T2	G3
	BT12	9.049	T1	G2
	BT15	8.579	T2	G3
	BT16	8.115	Ta	G2
	BT20	4.470	T1	G2
	BT21	5.192	Ta	G3
	BT22	2.973	T2	G2
	BT23	5.955	T1	G2
	BT28	11.206	Ta	G1
	BT31	11.773	Ta	G2
	BT32	4.400	T2	G3
	BT33	3.047	T1	G2
	BT34	4.440	Ta	G2
	BT35	2.559	T3a	G3
	BT36	4.644	T2	G3
	BT38	11.153	Ta	G2
	BT39	3.243	T1	G3
	BT40	2.226	T2	G3
	BT41	4.242	T1	G2
	BT42	4.386	T2	G3
	BT43	4.602	Ta	G1
	BT44	3.531	T1	G2
	BT46	5.698	Ta	G2
	BT48	9.216	T2	G3
	BT49	4.540	Ta	G1
	BT50	20.095	T1	G3
	BT51	11.250	Ta	G2
	BT52	3.960	T3	G3
	BT53	25.517	Ta	G2
	BT54	1.715	T1	G3
	BT56	9.261	T2	G3
	BT57	5.279	T1	G2
	BT58	8.787	Ta	G2
	BT59	3.478	T2	G3
	BT60	6.072	Mets	G3
	BT64	4.225	Ta	G2
	BT66	7.592	Ta	G1
	BT67	4.747	T1	G2
	BT68	3.240	Ta	G2
	BT69	48.947	Ta	G2
	BT70	3.020	T1	G2
	BT71	23.038	T1	G3
	BT72	26.930	Ta	G1
	BT74	23.278	Ta	G1
	BT76	2.813	T1	G1
	BT77	4.020	Ta	G2
	BT78	4.778	T1	G3
	BT79	2.940	Ta	G2
	BT80	2.602	Ta	G2
	BT81	3.880	Ta	G2
	BT82	2.980	T1	G3
	BT83	9.324	Ta	G2
	BT84	26.609	Ta	G2
	BT85	4.995	T1	G2
	BT87	1.266	T2	G2
	BT88	35.443	T1	G3
	BT90	5.981	Ta	G2
	BT92	3.308	T1	G2
	BT93	2.865	T2	G3
	BT94	6.183	Ta	G1
	BT95	2.875	T3a	G3
	BT96	2.054	Ta	G1
	BT97	4.208	Ta	G2
	BT98	27.254	Ta	G2
	BT99	7.847	T1	G2
	BT100	13.934	T1	G3
	BT101	4.923	T2	G3
	BT103	5.362	T1	G2
	BT104	2.362	T4	G2
	BT105	2.727	T2	G2
	BT106	7.263	Ta	G3
	BT107	4.899	Mets	G3
	BT108	7.960	T1	G2
	BT109	8.678	Ta	G2
	BT110	2.892	T1	G2
	BT112	8.352	Ta	G3
	BT113	5.914	T1	G3
	BT114	2.037	T2	G3
	BT115	1.517	T1	G3
	BT116	4.475	T2a	G3

Table 1. Clinicopathologic characterstics and [*LSD1*] expression (Continued)

Tissue	Sample name	*LSD1* expression	Stage	Grade
	BT119	2.528	Ta	G2
	BT120	15.045	Ta	G2
	BT122	3.270	T1	G3
	BT125	5.671	T1	G2
	BT128	14.005	Ta	G1
	BT129	9.751	Ta	G2
	BT130	7.160	Ta	G2
	BT131	4.316	T2	G3
	BT132	3.196	T2	G3
	BT133	3.714	T1	G2
	BT135	4.018	T2	G3
	BT137	2.990	Ta	G2
	BT138	3.546	Ta	G1
	BT139	9.191	T2	G3
	BT140	3.508	Ta	G2
	BT141	2.067	Mets	G3
	BT143	4.346	T1	G3
	BT145	2.424	T2	G2
	BT150	1.646	Ta	G2
	BT151	4.986	Ta	G3
	BT152	14.379	Ta	G2
	BT154	6.872	T1	G3
	BT158	7.466	Ta	G2
	BT160	3.763	T1	G2
	BT161	3.908	Ta	G2
	BT162	1.766	T3	G3
	BT164	6.602	Ta	G1
	BT165	2.156	T2	G3
	BT169	3.111	T2	G3
	BT178	2.778	Ta	G2
	BT180	2.177	T1	G2
	BT181	2.205	T2	G3
	BT187	4.937	Ta	G2
	BT188	40.158	T2	G3
	BT189	5.485	T1	G2
Normal bladder	BN11A	2.005		
	BN11B	2.313		
	BN12A	2.557		
	BN13A	1.833		
	BN14A	1.230		
	BN14B	2.256		
	BN15A	2.477		
	BN17B	2.412		

Table 1. Clinicopathologic characterstics and [*LSD1*] expression (Continued)

Tissue	Sample name	*LSD1* expression	Stage	Grade
	BN18	3.967		
	BN18B	3.098		
	BN19A	1.370		
	BN1A	2.835		
	BN20B	1.625		
	BN21A	3.392		
	BN22A	1.879		
	BN22B	1.773		
	BN25A	2.544		
	BN26A	1.737		
	BN2A	2.203		
	BN2B	2.113		
	BN4A	2.442		
	BN4B	2.439		
	BN5B	3.154		
	BN6A	3.900		
	BN8A	2.150		
	BN9A	3.291		

intensity ranges with the midpoints being at $\log_2((\text{intensity}_1 + \text{intensity}_2)/2) = 5, 7, 9, 11, 13$ and 15. We modeled intensity variation using the formula $\text{stdev}(\log_2(\text{intensity}_2/\text{intensity}_1)) = a^* (\log_2((\text{intensity}_1 + \text{intensity}_2)/2)) + b$ and estimated parameters a and b using the method of least squares. Using these values, the standard deviation of intensity fluctuation was calculated. The signal intensities of each probe were then compared between siLSD1 (EXP) and controls (siEGFP/siFFLuc) (CONT) and tested for up/downregulation by calculating the z-score: $\log_2(\text{intensity}_{EXP}/\text{intensity}_{CONT})/(a^* (\log_2((\text{intensity}_{EXP} + \text{intensity}_{CONT})/2)) + b)$. Resultant p-values for the replication sets were multiplied to calculate the final p-value of each probe. These procedures were applied to each comparison: siEGFP *vs.* siLSD1, siFFLuc *vs.* siLSD1 and siEGFP *vs.* siFFLuc, respectively. We determined up/downregulated gene sets as those that simultaneously satisfied the following criteria: (*i*) The Benjamini-Hochberg false discovery rate (FDR) ≤ 0.05 for siEGFP *vs.* siLSD1, (*ii*) FDR ≤ 0.05 for siFFLuc *vs.* siLSD1 and the regulation direction is the same as (*i*) and (*iii*) siEGFP *vs.* siFFLuc has the direction opposite to (*i*) and (*ii*) or $p > 0.05$ for siEGFP *vs.* siFFLuc. Finally, we performed a pathway analysis using the hypergeometric distribution test, which calculates the probability of overlap between the up/downregulated gene set and each GO category compared against another gene list that is randomly sampled. We applied the test to the identified up/downregulated genes to test whether or not they are significantly

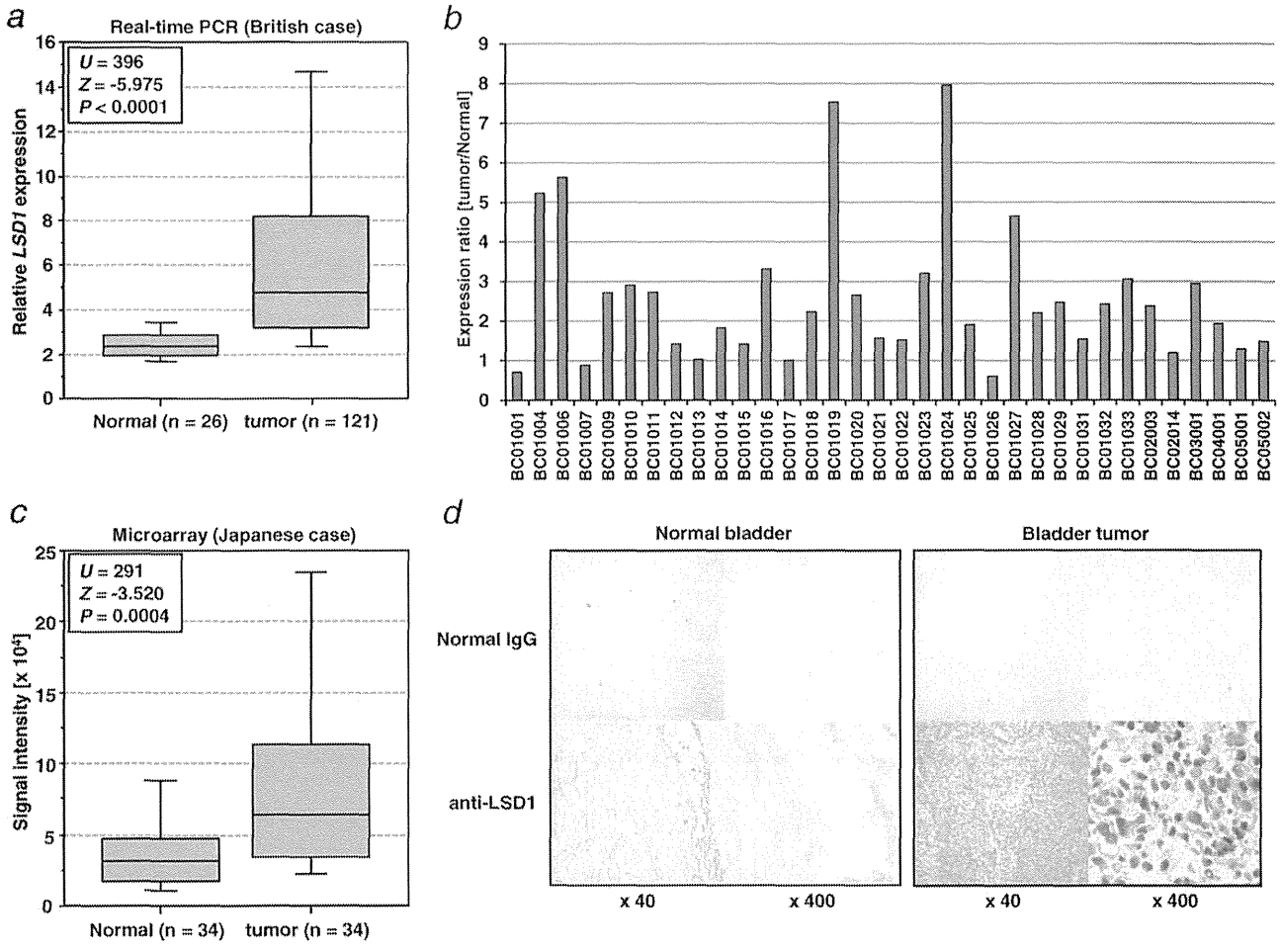

Figure 1. Elevated *LSD1* expression in bladder cancer in British and Japanese patients. (*a*) *LSD1* gene expression in normal and tumor bladder tissues in British cases. Expression levels of *LSD1* were analyzed by quantitative real-time PCR, and the result is shown by box-whisker plot (median 50% boxed). Mann-Whitney's *U*-test was used for statistical analysis. (*b*) Expression ratio between normal and tumor bladder tissues from Japanese patients. Signal intensity for each sample was analyzed by cDNA microarray, and the expression ratio is the signal intensity in tumor divided by that in normal (1 = normal). (*c*) Comparison of *LSD1* expression in normal and tumor bladder tissues in Japanese patients. Signal intensity of each sample was analyzed by cDNA microarray, and the result is shown by box-whisker plot. Mann-Whitney's *U*-test was used for the statistical analysis. (*d*) Immunohistochemical staining of LSD1 in bladder tissues. Nonimmunized rabbit IgG was used as a negative control. Original magnification, ×40 (left panels) and ×400 (right panels).

enriched (FDR $\leq$ 0.05) in each category of "biological processes" (857 categories) as defined by Gene Ontology database.

Results

LSD1 expression is upregulated in clinical cancer tissues

We first examined expression levels of various histone demethylase genes involved, demethylase candidate genes, which possess JmjC domain, in 121 bladder cancer samples and 26 normal control samples obtained in the UK, and found significant elevation of *LSD1* expression in tumors compared with in normal tissues ($p < 0.0001$, Mann-Whitney's *U*-test) (Table 1 and Fig. 1*a*). As shown in Table 2, there was no significant correlation of *LSD1* expression with clinical and pathological features (gender, smoking histroy, grading, metastatic status and recurrence status), suggesting the involvement of *LSD1* transactivation from an early stage of bladder carcinogenesis. Importantly, expression levels of *LSD1* were significantly high even in tumors at an early grade (G1), indicating that *LSD1* may be one of the factors involved in the initiation process of carcinogenesis. We then analyzed the expression patterns of *LSD1* in a number of Japanese clinical bladder cancer samples by cDNA microarray (Fig. 1*b*) and confirmed significant overexpression in bladder cancers of Japanese patients ($p = 0.0004$, Mann-Whitney's *U*-test, Fig. 1*c*). To evaluate protein expression levels of LSD1 in bladder tissues, we performed immunohistochemical analysis using an anti-LSD1 antibody and detected strong LSD1 staining, mainly in the nucleus of malignant

Table 2. Statistical analysis of *LSD1* expression levels in clinical bladder tissues

		LSD1		
Factor	Case (*n*)	Mean	SD	95% CI
Normal (Control)	26	2.423	0.710	2.137–2.710
Tumor (Total)	121	7.435	7.792	6.033–8.838
Gender				
Male	88	8.239	8.624	6.412–10.067
Female	31	5.240	4.468	3.601–6.879
Smoked				
No	27	6.273	3.602	4.848–7.698
Yes	50	8.906	9.909	6.028–11.783
Grade				
G1	12	9.447	8.113	4.292–14.601
G2	61	7.370	7.820	5.366–9.370
G3	47	7.008	7.856	4.701–9.314
Metastasis				
Negative	94	7.495	8.050	5.846–9.144
Positive	27	7.227	6.956	4.475–9.979
Recurrence				
No	26	9.136	9.783	5.184–13.087
Yes	50	7.784	8.570	5.349–10.220
Died	8	7.748	8.672	0.499–14.998

cells, while low staining was observed in any of nonneoplastic tissues (Fig. 1*d*). In addition, we examined microarray expression analysis of a large number of clinical samples derived from Japanese subjects and found that *LSD1* expression was also significantly upregulated in small cell lung cancer and colorectal cancer tissues compared with corresponding nonneoplastic tissues ($p < 0.0001$, $p = 0.0009$, respectively, Fig. 2), indicating its possible involvement in many types of human cancer.

Growth regulation of cancer cells by LSD1

To investigate roles of LSD1 in human carcinogenesis, we performed a knockdown experiment using 2 independent siRNAs targeting *LSD1* (siLSD#1 and #2). First, we examined *LSD1* expression in various bladder and lung cancer cell lines and compared the expression level to that in normal bladder and lung tissues (Fig. 3*a*). Expression levels of *LSD1* in bladder and lung cancer cell lines were significantly higher than those in normal bladder and lung tissues. In addition, *LSD1* expression in A549 and SBC5 cells transfected with siLSD1#1 and #2 was significantly suppressed compared to that transfected with control siRNAs, siEGFP or siNegative control (Fig. 3*b*). We also confirmed the knockdown effect at the protein level (Fig. 3*c*). Using the same siRNAs, we performed cell growth assays in 2 bladder cancer cell lines (SW780, RT4) and 3 lung cancer cell lines (A549, LC319 and SBC5) and found significant growth suppression by the siLSD1. No growth-suppressive effect was observed when we used 2 control siRNAs (Fig. 3*d*). We further validated the effect of siRNAs targeting LSD1 on the growth of noncancerous HEK293 cells and found no significant effect on the growth of cancer cells, although we used the same condition to suppress the growth of cancer cells (Supporting Information Fig. 2*a*). Moreover, we performed a genetic rescue experiment by restoring LSD1 expression with transfection of the LSD1 expression vector in the knockdown cells. We transfected a pCAGGSn3FC control vector (Mock) or a pCAGGSn3FC-LSD1 expression vector for restoring LSD1 expression at 24 hr after treatment with siLSD1 and performed the growth assay at 48 hr after transfection of pCAGGS vectors. As shown in Supporting Information Figure 2*b*, the growth of SBC5 cell lines appears to be recovered after restoring LSD1 expression compared with mock-transfected cells. The data support that the growth suppression of cancer cells after treatment with siRNAs was not the off-target effects but specific effect by knockdown of LSD1.

To elucidate the mechanism how LSD1 upregulation influences to the growth of cancer cells, we examined the effect of LSD1 overexpression using HEK293 cells containing the Flp-In™ T-REx™ system (T-REx™ 293, Invitrogen). The V5-tagged LSD1 expression vector, empty vector (mock) or V5-tagged CAT expression vector (control) were transfected into the T-REx 293 cells to establish stable cell lines expressing LSD1. LSD1 proteins in the T-REx-LSD1 cells were mainly located in the nucleus (Supporting Information Fig. 1*b*). We analyzed the cell cycle status by FACS analysis (Fig. 3*e*) and found that the proportions at the S phase were slightly but significantly increased in the T-REx-LSD1 cells compared with those in the control cells ($p = 0.0055$ [Mock, LSD1] and $p = 0.0026$ [CAT, LSD1], respectively). Conversely, the proportion at the G_0/G_1 phase in the T-REx-LSD1 cells was slightly lower than that in the control cells ($p = 0.0006$ [Mock, LSD1] and $p = 0.0003$ [CAT, LSD1], respectively). We also performed BrdU and 7-AAD staining to analyze the detailed cell cycle status of cancer cells and confirmed that the proportion of cancer cells at the S phase was significantly decreased after the knockdown of LSD1 (Fig. 3*f*). Furthermore, we measured caspase-3 activity in the cancer cells treated with siRNAs and found no significant effect on it. These results imply that LSD1 expression plays an important role in the growth of cancer cells through enhancement of the cell cycle progression, and the inhibition of LSD1 could suppress the G_1 to S progression without induction of caspase-mediated apoptosis cancer cells.

Identification of the downstream genes by microarray expression analysis

To identify signal pathways downstream to LSD1, we performed microarray expression analysis. After knocking down of LSD1 in SW780 and A549 cancer cells, we isolated total RNA from SW780 and A549 24 hr after the treatment with siLSD1#1. The expression profiles of these cells were compared to the cells treated with control siRNAs (siEGFP and siFFLuc) using Affymetrix HG-U133 Plus 2.0 Array. Expression of 198

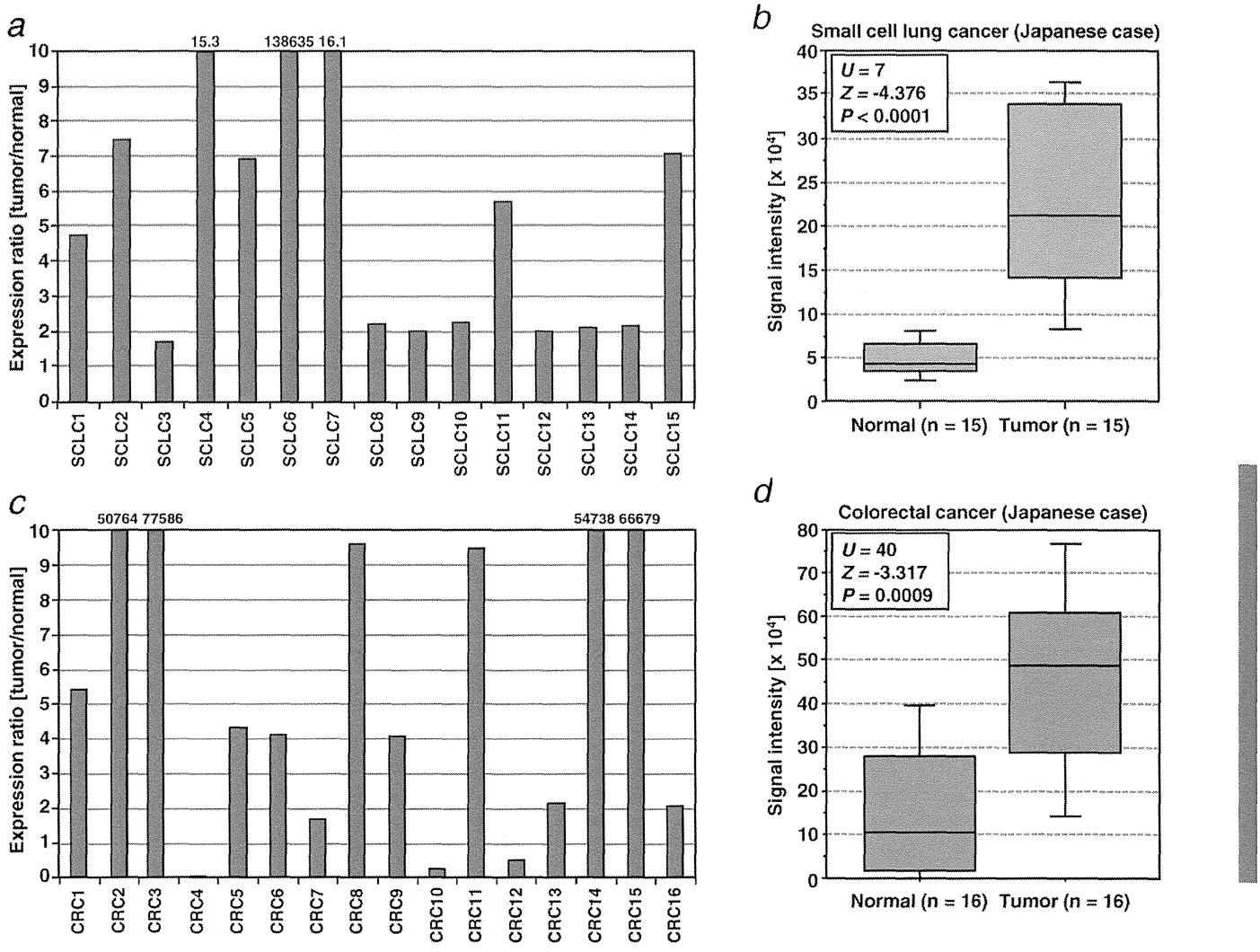

Figure 2. Elevated *LSD1* expression in lung and colorectal cancer in Japanese patients. (*a*) Expression ratio of *LSD1* between small cell lung cancer (SCLC) tissue samples and corresponding normal lung tissues. cDNA microarray signal intensity for each sample was analyzed, and tumor/normal expression ratio is shown (1 = normal). (*b*) Comparison of *LSD1* expression between normal and tumor lung tissues in Japanese patients. Signal intensity of each sample was analyzed by cDNA microarray, and the result is shown by box-whisker plot. Mann-Whitney's *U*-test was used for the statistical analysis. (*c*) Expression ratio (tumor/normal) for colorectal tissue samples. Signal intensity for each sample was analyzed by cDNA microarray, and the expression ratio is the signal intensity in tumor divided by that in normal (1 = normal). (*d*) Comparison of *LSD1* expression between normal and tumor colorectal tissues in Japanese patients. Signal intensity of each sample was analyzed by cDNA microarray, and the result is shown by box-whisker plot (median 50% boxed). Mann-Whitney's *U*-test was used for the statistical analysis.

genes decreased and 72 genes increased statistically by the knockdown of LSD1, so these 270 genes were suggested to be the downstream genes affected by knockdown of LSD1 (Supporting Information Fig. 3). Because we were able to validate the downregulation of several randomly selected downstream gene candidates (Supporting Information Fig. 4), our microarray data must be reproducible.

Signal pathway analysis for determining the downstream candidates using the Gene Ontology database (Material and Methods; Table 3) indicated that LSD1 could regulate a wide variety of chromatin functions, including chromatin remodeling at centromere, centromeric heterochromatin formation and chromatin assembly or disassembly and methylation-dependent chromatin silencing. Therefore, dysfunction of LSD1 expression is likely to contribute to human carcinogenesis partially through these chromatin regulations.

Discussion

Histone modifications, including methylation, acetylation, phosphorylation and ubiquitination, are considered to play

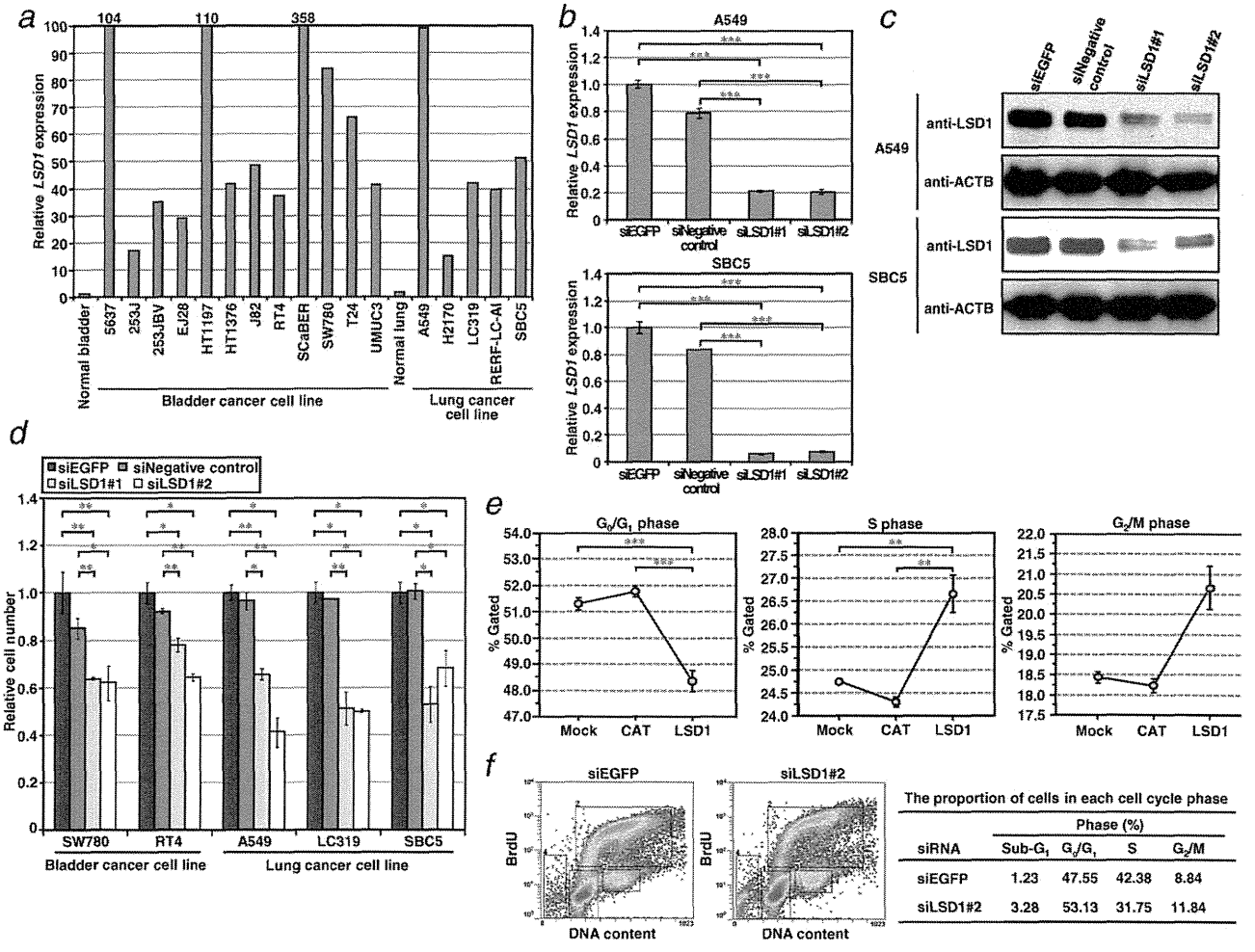

Figure 3. Involvement of LSD1 in the growth of bladder and lung cancer cells. (*a*) Expression of *LSD1* in normal bladder tissue, normal lung tissue, 12 bladder cancer cells and 5 lung cancer cells. Expression levels of *LSD1* were analyzed by quantitative real-time PCR. Data were normalized by *GAPDH* and *SDH* expressions, and relative LSD1 expression shows the ratio compared to the value in normal bladder tissue (1 = normal bladder tissue). (*b*) Quantitative real-time PCR showing suppression of endogenous *LSD1* expression by 2 independent LSD1-specific siRNAs (siLSD1#1, #2) in A549 and SBC5 cells. siRNA targeting *EGFP* (siEGFP) and siNegative Control (B-Bridge International) were used as controls. mRNA expression levels were normalized by *GAPDH* and *SDH* expressions, and values are relative to siEGFP (siEGFP = 1). Results are the mean ± SD of 3 independent experiments. *p*-values were calculated using Student's *t*-test (***$p < 0.001$). (*c*) Validation of LSD1 expression at the protein level. Lysates from A549 and SBC5 cells after siRNA treatment were immunoblotted with anti-LSD1 and ACTB antibodies. Expression of ACTB served as a control. (*d*) Effect of *LSD1* siRNA knockdown on the viability of bladder cancer cell lines (SW780 and RT4) and lung cancer cell lines (A549, LC319 and SBC5). Relative cell numbers are normalized to the number of siEGFP-treated cells (siEGFP = 1): results are the mean ± SD of 3 independent experiments. *p*-values were calculated using Student's *t*-test (*$p < 0.05$; **$p < 0.01$). (*e*) Numerical analysis of the FACS result, classifying cells by cell cycle status. The proportion of T-REx-LSD1 cells in S and G_2/M phases is slightly higher than control cells (T-REx-Mock and T-REx-CAT). Mean ± SD of 3 independent experiments. Fisher's PLSD *post hoc* test was used to calculate *p*-values (**$p < 0.01$; ***$p < 0.001$). (*f*) Effect of siLSD1 on cell cycle kinetics in SBC5 cells. Cell cycle distribution was analyzed by flow cytometry after coupled staining with fluorescein isothiocyanate (FITC)-conjugated anti-BrdU and 7-amino-actinomycin D (7-AAD) as described in Material and Methods.

critical roles in transcriptional activation and repression through the regulation of chromatin structure. Histone methylation had been thought to be a stable modification, but is at present considered to be dynamically regulated by both histone methyltransferases and demethylases. LSD1, the first one to be identified as a histone lysine demethylase, uses an amine oxidase reaction to catalyze the removal of methyl groups.[1] This study has demonstrated that LSD1 was significantly upregulated in bladder cancer, by real-time PCR, microarray data and immunohistochemistry. Our microarray analysis also indicated LSD1 to be aberrantly overexpressed in lung and colorectal cancers. It was reported that LSD1 was